USGS
science for a changing world

Prepared in cooperation with the U.S. Army Corps of Engineers and Levee Ready Columbia

Assessment of Columbia and Willamette River Flood Stage on the Columbia Corridor Levee System at Portland, Oregon, in a Future Climate

Scientific Investigations Report 2018–5161

U.S. Department of the Interior
U.S. Geological Survey

Cover: Photograph showing Willamette Falls on Willamette River looking downstream.
Photograph by U.S. Army Corps of Engineers, February 1996.

Assessment of Columbia and Willamette River Flood Stage on the Columbia Corridor Levee System at Portland, Oregon, in a Future Climate

By Susan A. Wherry, Tamara M. Wood, Hans R. Moritz, and Keith B. Duffy

Prepared in cooperation with the U.S. Army Corps of Engineers
and Levee Ready Columbia

Scientific Investigations Report 2018–5161

U.S. Department of the Interior
U.S. Geological Survey

U.S. Department of the Interior
DAVID BERNHARDT, Acting Secretary

U.S. Geological Survey
James F. Reilly II, Director

U.S. Geological Survey, Reston, Virginia: 2019

For more information on the USGS—the Federal source for science about the Earth, its natural and living resources, natural hazards, and the environment—visit https://www.usgs.gov or call 1–888–ASK–USGS.

For an overview of USGS information products, including maps, imagery, and publications, visit https://store.usgs.gov.

Suggested citation:
Wherry, S.A., Wood, T.M., Moritz, H.R., and Duffy, K.B., 2019, Assessment of Columbia and Willamette River flood stage on the Columbia Corridor Levee System at Portland, Oregon, in a future climate: U.S. Geological Survey Scientific Investigations Report 2018-5161, 44 p., https://doi.org/10.3133/sir20185161.

ISSN 2328-0328 (online)

Contents

Figures

Tables

Conversion Factors

Inch/Pound to International System of Units

Multiply	By	To obtain
	Length	
mile (mi)	1.609	kilometer (km)
	Area	
square mile (mi^2)	2.590	square kilometer (km^2)

International System of Units to U.S. customary units

Multiply	By	To obtain
	Length	
centimeter (cm)	0.3937	inch (in.)
meter (m)	3.281	foot (ft)
kilometer (km)	0.6214	mile (mi)
	Area	
square kilometer (km^2)	247.1	acre
square kilometer (km^2)	0.3861	square mile (mi^2)
	Volume	
cubic kilometer (km^3)	0.2399	cubic mile (mi^3)
cubic meter (m^3)	0.0008107	acre-foot (acre-ft)
	Flow rate	
cubic meter per second (m^3/s)	35.31	cubic foot per second (ft^3/s)
cubic meter per second per square kilometer ($[m^3/s]/km^2$)	91.49	cubic foot per second per square mile ($[ft^3/s]/mi^2$)

Temperature in degrees Celsius (°C) may be converted to degrees Fahrenheit (°F) as

$$°F = (1.8 \times °C) + 32.$$

Datums

Vertical coordinate information is referenced to the North American Vertical Datum of 1988 (NAVD 88) unless indicated otherwise in the text.

Mean lower low water (MLLW) is calculated at Astoria, Oregon, during the 1983–2001 epoch.

Mean sea level is calculated at Astoria, Oregon, during the 1983–2001 epoch and is 1.37 m (4.51 ft) above MLLW.

The Columbia River Datum (CRD) plane for areas downstream of Harrington Point, Washington, is based on MLLW. Upstream of Harrington Point to Bonneville Dam, zero CRD roughly corresponds to the river level at minimum operating discharge from Bonneville Dam (2000 m^3/s [70,000 ft^3/s]). Zero CRD at Vancouver, Washington (RM 105), is equal to -1.6 m (-5.3 ft) NAVD 88 and zero CRD at Skamokawa, Washington, is equal to -0.4 m (-1.4 ft) NAVD 88.

Horizontal coordinate information is referenced to the North American Datum of 1983 (NAD 83).

Abbreviations

AdH	Adaptive Hydraulics
AEP	annual exceedance probability hydraulics model
CIG	Climate Impacts Group
CMIP	Coupled Model Intercomparison Project
Delft3D-FM	Delft3D-Flexible Mesh model
FEM	finite element method
FEMA	Federal Emergency Management Agency
GCM	general circulation model
GEBCO	General Bathymetric Chart of the Oceans
LCR	lower Columbia River
LRC	Levee Ready Columbia
MCDD	Multnomah County Drainage District No. 1
MCR	mouth of the Columbia River
MOVE.1	Maintenance Of Variance-Extension, type 1
MSL	mean sea level
NOAA	National Oceanic and Atmospheric Administration
PEN 1	Peninsula Drainage District No. 1
PEN 2	Peninsula Drainage District No. 2
RM	river mile
RMJOC	River Management Joint Operating Committee
RMSE	root mean squared error
SDIC	Sandy Drainage Improvement Company
SLC	sea-level change
SREF	Streamflow Record Extension Facilitator
SRES	Special Report on Emissions Scenarios
USACE	U.S. Army Corps of Engineers
USGS	U.S. Geological Survey

Assessment of Columbia and Willamette River Flood Stage on the Columbia Corridor Levee System at Portland, Oregon, in a Future Climate

By Susan A. Wherry[1], Tamara M. Wood[1], Hans R. Moritz[2], and Keith B. Duffy[2]

Abstract

To support Levee Ready Columbia's (LRC's) effort to re-certify levees along the Columbia and Willamette Rivers and remain accredited, two 2-dimensional hydraulic models, Adaptive Hydraulics and Delft3D-Flexible Mesh, were used to simulate the effects of plausible extreme high water during the 2030 to 2059 period. The Columbia River was simulated from Bonneville Dam, situated at river mile (RM) 145, to the mouth of Columbia River, and the Willamette River was simulated from Willamette Falls, RM 26.2, to the Columbia River confluence. Inputs to the models included light detection and ranging (lidar) and bathymetric mapping data to determine bed level, and boundary conditions in the form of daily inflow hydrographs and water levels in the ocean offshore of the mouth of the Columbia River.

Future conditions were based on climate science data developed by the U.S. Army Corps of Engineers and others. These conditions included future streamflow and coastal ocean water levels. The hypothetical, extreme but plausible, upstream boundary was based on scaling up the hydrographs from the 1996 flood. Scaling factors were determined by comparing the peak flow rankings determined from flood frequency analyses of historical unregulated periods and 2040s simulated unregulated winter streamflow. The comparison resulted in scaling up the Columbia River hydrograph by 40-percent and scaling up the Willamette River and Lower Columbia River tributaries hydrographs by 20-percent. The downstream ocean boundary was based on a combination of sea-level change, high tide, and storm surge.

The models were calibrated for two historical periods: (1) from January 15 to February 28, 1996, and (2) from April 12 to July 12, 1997. The two models compared well to the measured water-surface elevation over the historical periods and had good performance statistics, with root-mean square error ranging from 0.085 to 0.32 meters, Nash-Sutcliffe values greater than 0.96, and bias ranging from -0.03 to 0.28 meters. The simulated peak stage in the Columbia River at Vancouver, Washington, for 1996 was 9.60 and 9.98 meters (31.5 and 32.7 feet) compared to the measured peak of 9.89 meters (32.5 feet). Future peak stage then was simulated with boundary conditions representing extreme but plausible future conditions at the inflow sites and the ocean boundary.

The two calibrated models compared well in their simulations of extreme but plausible future conditions. For the 0-meter sea-level change scenario, the simulated peak stage in the Columbia River at Vancouver was 11.15 and 11.39 meters (36.6 and 37.4 feet); and for the 1-meter sea-level change scenario, the simulated peak stage in the Columbia River was 11.25 and 11.54 meters (36.9 and 37.9 feet). The total increase in stage as compared to the 1996 measured peak stage ranged from 1.26 to 1.65 meters (4.13 to 5.40 feet).

Significant Findings

1. Two 2-dimensional hydraulic models were calibrated to historical high-flow periods in 1996 and 1997. The models compared well in simulating the timing and magnitude of river stage in the Columbia and Willamette Rivers near Portland, Oregon.

2. Winter rain-on-snow periods were postulated to be a likely cause of future extreme flooding events in addition to the spring freshet, which the Columbia River system of dams best regulates. The 1996 flood period was selected as a historical, extreme, rain-on-snow winter period to scale up for simulating future climate.

    - Extreme but plausible winter increases in flow were simulated as 40-percent on the Columbia River and 20-percent on the Willamette River, based on the selection of a moderately wet and warm general circulation model, and a moderate scenario for future greenhouse gas emissions.

[1]U.S. Geological Survey.

[2]U.S. Army Corps of Engineers.

3. Storm surges could have a significant effect on tidal boundaries and upstream stage depending on the peak timing. Historical storm surges increased tidal stage by as much as 1.68 meters (5.51 feet), which is higher than the maximum potential relative sea-level rise attributable to climate change through the year 2100 at Astoria, Oregon, as provided by U.S. Army Corps of Engineers guidance.

4. The models using extreme but plausible future hydrographs simulated increases in stage of 1.26 to 1.65 meters (4.13 to 5.40 feet) relative to the 1996 measured peak stage in the Portland area. Additionally, most levees will be subject to prolonged exposure from water levels that exceed the safe levee height, which is defined by the U.S. Army Corps of Engineers as the highest flood level for which reasonable flood protection is provided.

Introduction

Levee Ready Columbia (LRC), a partnership of more than 20 organizations committed to collaborative and proactive flood risk reduction, is working to recertify the Columbia corridor levee system (CCLS) to ensure accreditation by meeting the Federal Emergency Management Agency (FEMA) and U.S. Army Corps of Engineers (USACE) Federal standards. LRC has taken a proactive approach to the recertification and accreditation process for these levees, and has requested assistance assessing the potential effects of a changing climate on the Columbia and Willamette River water levels near Portland and on sea level downstream at the mouth of the Columbia River (MCR). The U.S. Geological Survey (USGS) and USACE proposed to provide this assistance in the form of hydraulic model simulations of the lower Columbia River (LCR; fig. 1). This modeling incorporates the best available knowledge at the time of this study regarding peak flows in the Columbia and Willamette Rivers in a future climate, and projected sea-level change (SLC) at the MCR, both of which affect river stage at Portland.

This study focused on assessing future flood stage on the CCLS, which consists of 72 kilometers ([km] 45 miles [mi]) of levees near the fluvially dominated convergence of the Columbia and Willamette Rivers, and spans the southern shore of the Columbia River from North Portland near the Smith and Bybee Wetlands Natural Area to the Sandy River. The system is managed by three drainage districts and one drainage improvement company: Peninsula Drainage District #1 (PEN 1), Peninsula Drainage District #2 (PEN 2), Multnomah County Drainage District #1 (MCDD), and Sandy Drainage Improvement Company (SDIC; fig. 2).

Throughout the report, variables are presented in the International System (SI) of Units with inch/pound units in parentheses to accommodate the wide range of readers interested in the CCLS. The only exceptions are the Columbia River mile demarcations, which are presented only in inch/pound units, and the sea-level change increments used for the future simulations, which are only presented in SI units.

Hydrology and Morphology of the Lower Columbia River

The Columbia River flows into the Pacific Ocean at the boundary between Oregon and Washington after traversing 1,990 km (1,240 mi), dropping over 790 meters ([m] 2,600 feet [ft]) from its Canadian headwaters in the Rocky Mountains, and draining an area of approximately 668,000 square kilometers ([km^2] 258,000 square miles [mi^2]). The Columbia River is the second largest river in the United States in terms of annual river discharge; its drainage basin accounts for 60 percent of the total freshwater discharge into the Pacific Ocean between the Canadian border and San Francisco, California, during winter, and 90 percent during summer. The drainage area for the Lower Columbia River (LCR) downstream of Bonneville Dam (river mile [RM] 145) is about 52,000 km^2 (about 20,000 mi^2), including the Willamette River Basin, and composes less than 10 percent of the overall Columbia River Basin. However, the LCR drainage area is an important part of the fluvial input to the lower river. Average runoff for the LCR drainage area is 0.0398 cubic meters per second per square kilometer ([m^3/s]/km^2) (3.62 [ft^3/s]/mi^2), whereas average run-off from the drainage area upstream of Bonneville Dam is only 0.0089 (m^3/s)/km^2 (0.82 [ft^3/s]/mi^2) (Orem, 1968). The high runoff contribution for the LCR drainage is associated with west Cascades Range hydrology, which is dominated by the Willamette River Basin during autumn to spring, and explains the relevance of the Willamette River in terms of its effect on the combined flow for the LCR. The high runoff contribution produces flooding of non-leveed areas, and threatens levee systems along the LCR. The Willamette River flows into the LCR at Portland (RM 101). Other prominent LCR tributaries include the Cowlitz River (RM 68) and Lewis River (RM 87), Washington, Sandy River (RM 121), Oregon, and Washougal River (RM 121), Washington, which were included in the model boundaries to ensure completeness.

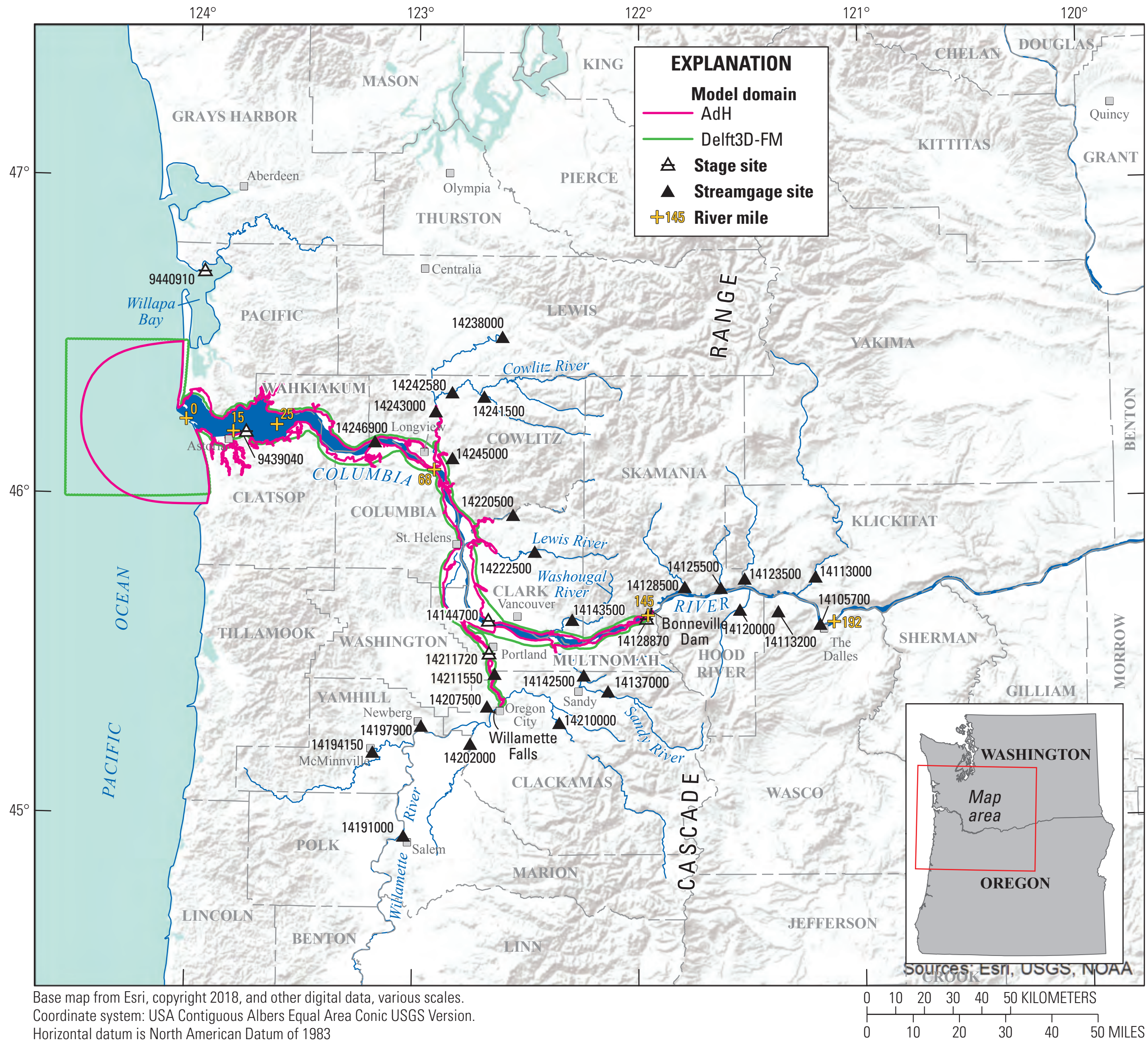

Figure 1. Locations of model domains and measurement sites along the Columbia and Willamette Rivers near Portland, Oregon. Site information is shown in table 2.

The Columbia River estuary is the largest fluvially dominated estuary in the Pacific Northwest (Fox and others, 1984). It has a tidal prism, the difference in volume between low and high tide, of about 1.1 cubic kilometers (km^3) (890,000 acre-ft; Jarrett, 1976). Freshwater inflows to the estuary primarily are from the Columbia and Willamette Rivers, and range from a late summer combined low of 2,200 cubic meters per second (m^3/s) (78,000 cubic feet per second [ft^3/s]) to an annual spring freshet of 8,500 m^3/s (300,000 ft^3/s). The 0.01 annual exceedance probability (AEP) event for regulated river flow passing The Dalles Dam (RM 192) is about 19,000 m^3/s (670,000 ft^3/s) with about 840 m^3/s (30,000 ft^3/s) in tributary inflows entering the Columbia River between The Dalles and Bonneville Dam (U.S. Army Corps of Engineers, 1991). The 0.01 AEP regulated flow for the Willamette River at Willamette Falls (26 mi upstream of the confluence with the Columbia River) is about 11,000 m^3/s (390,000 ft^3/s; U.S. Army Corps of Engineers, 1991).

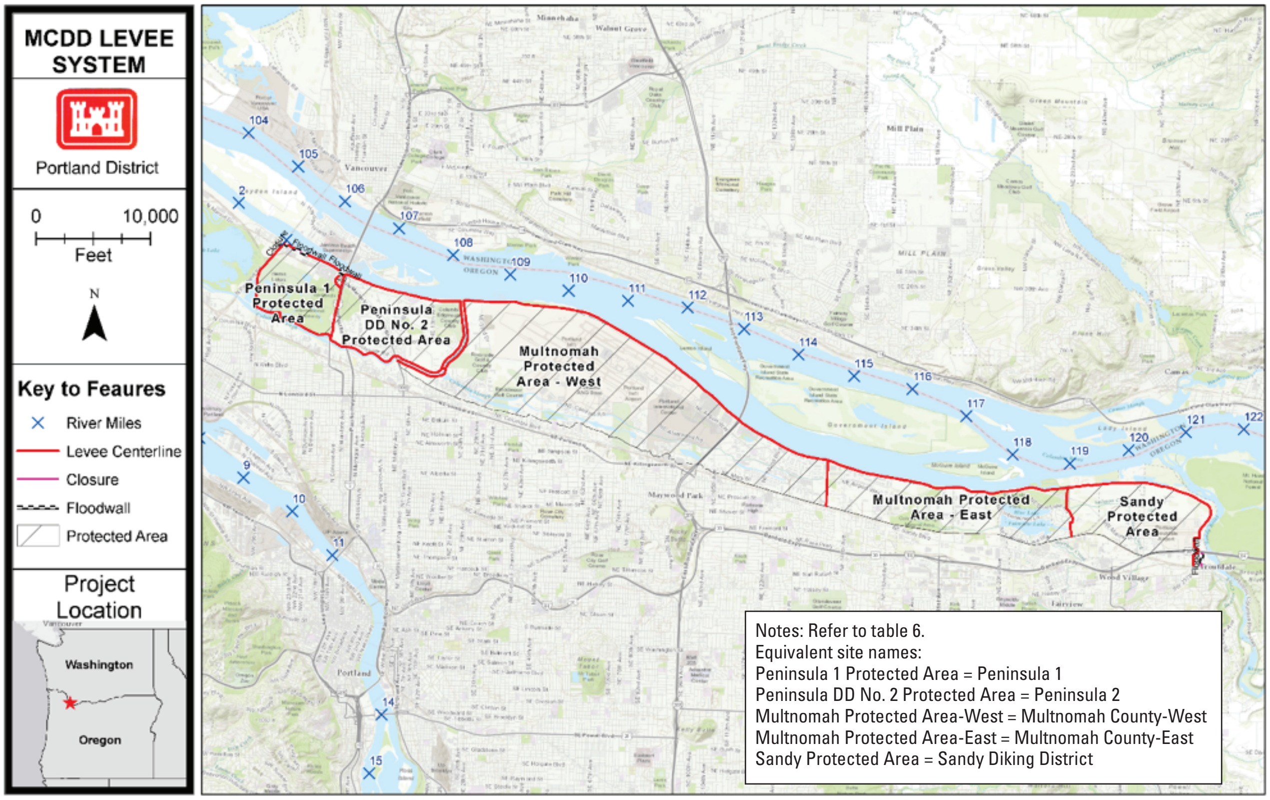

Map from U.S. Army Corps of Engineers, 2018

Figure 2. Columbia corridor levee system including locations of drainage district areas and drainage improvement company area near Portland, Oregon.

Downstream of RM 38, the LCR estuary consists of multiple deep channels meandering past shallow tidal flats, sandbars, and islands within a wide coastal plain (fig. 3). LCR tides in the estuary are of the mixed type with two high and two low water levels per day. The diurnal tide range at Astoria, Oregon (RM 15) is about 2.6 m (8.5 ft) and is 0.3 m (1.0 ft) larger than the MCR (RM 0) due to tidal amplification within the estuary. The upriver limit for the Columbia River estuary, defined in terms of salt water intrusion, varies between RMs 28 and 38 and is a function of fluvial flow and timing of the tidal cycle (Simenstad and others, 2011). The hydraulic forcing for the lower estuary (downstream of RM 38) is correlated with tidal phase.

Depending on the discharge magnitude, fluvial discharge increasingly controls river hydraulics moving upstream from RM 38. During times of low river flow (less than about 7,100 m^3/s [251,000 ft^3/s]), tidal propagation can cause reversal of the current throughout the water column in the Willamette River at locations more than 16 km (10 mi) upstream of the confluence with the Columbia River (RM 101; fig. 4). Tidal effects on water-surface elevation in the Columbia River extend upriver to Bonneville Dam (RM 145). During times of low river flow, a high tide entering the Columbia River from the Pacific Ocean takes about 5.5 hours to progress up the Columbia River from Astoria (RM 15) to the confluence of the Willamette River (RM 101).

Upstream of RM 38 (northern end of Puget Island; fig. 3), the LCR morphology becomes constrained by confining geology, leveed flood plain, and navigation improvements. This confining effect of the LCR produces a single river thalweg with a relatively steep profile gradient, compared to the lower estuary. Much of the expansive flood plain along RMs 80–124 has been leveed to decrease potential flood damage in low-lying areas during high river flow conditions, further confining the river and increasing river stage during extreme flow events (fig. 4). Upstream of the Sandy River (RM 121) the LCR is confined by the Columbia River Gorge through the Cascade Range (fig. 1).

Progressive improvement of the LCR for navigation has produced a navigation channel from the MCR to Vancouver, Washington (RM 105) about 183 m (600 ft) wide and maintained to an authorized depth of 13.1 m (43 ft) below Columbia River Datum (CRD), a datum based on river water level during minimum operating discharge from Bonneville

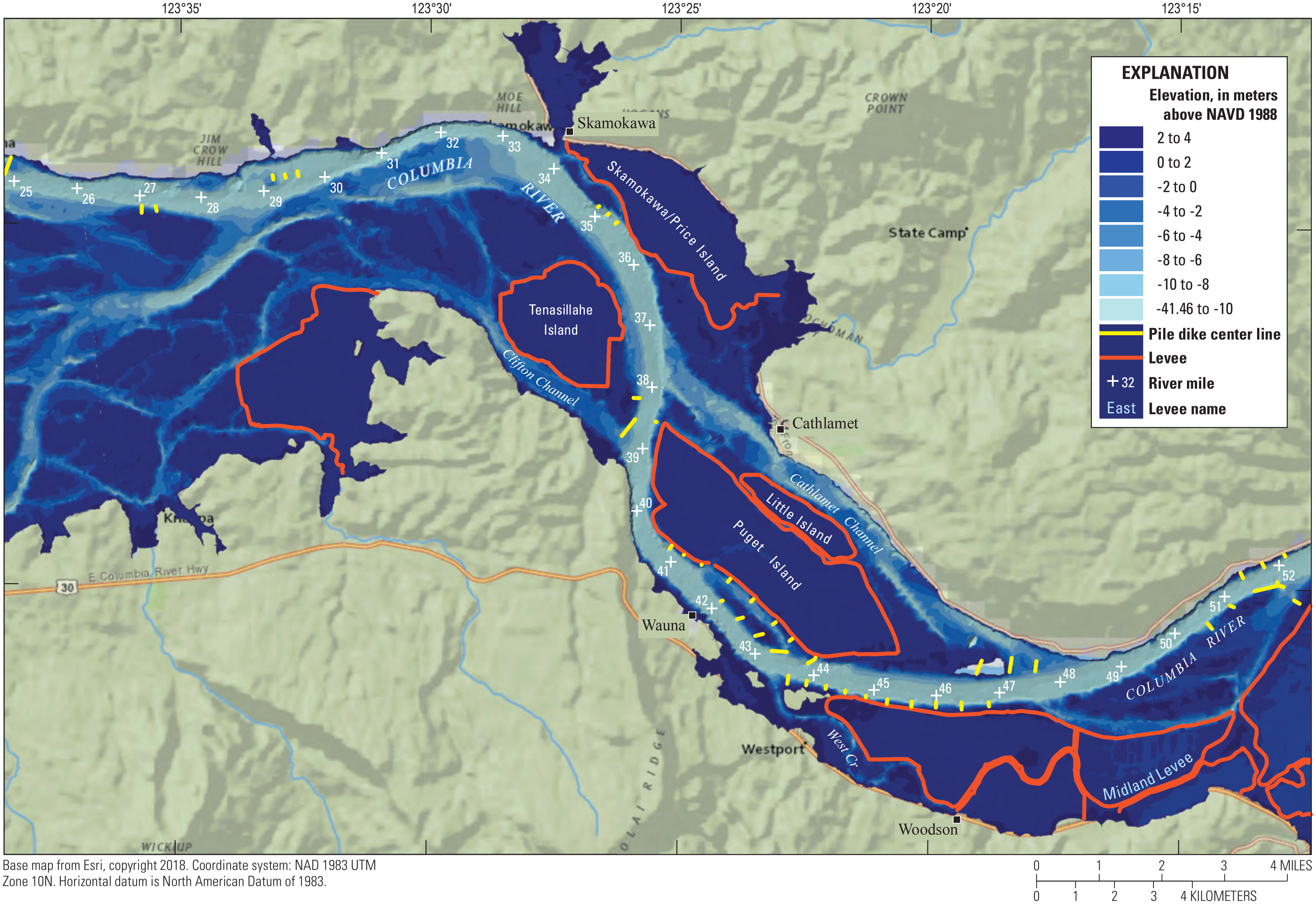

Base map from Esri, copyright 2018. Coordinate system: NAD 1983 UTM Zone 10N. Horizontal datum is North American Datum of 1983.

Figure 3. Land-surface elevations, levees, and pile dikes in the Columbia River for river miles 28 to 48, near Astoria, Oregon.

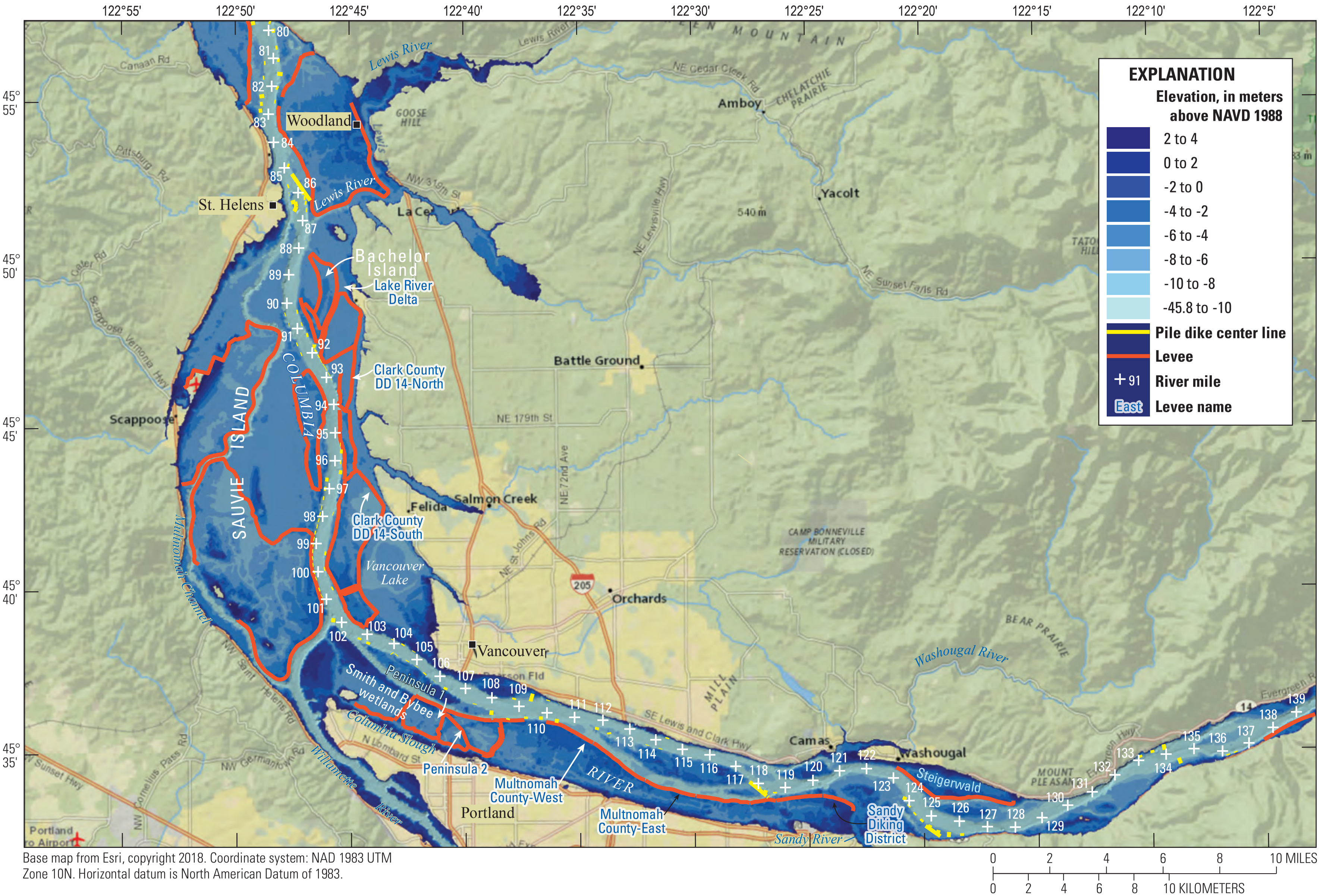

Base map from Esri, copyright 2018. Coordinate system: NAD 1983 UTM Zone 10N. Horizontal datum is North American Datum of 1983.

Figure 4. Land-surface elevations, levees, and pile dikes near the confluence of the Columbia and Willamette Rivers and near Multnomah County Drainage District levees, Portland, Oregon.

Dam. From RM 105 to Bonneville Dam (fig. 1), the navigation channel is 91 m (300 ft) wide and maintained at 5.2 m (17 ft) below CRD. Construction of 233 pile dikes (flow-control structures) along the LCR has improved navigation reliability by stabilizing river banks and islands and has further confined river flow to the channel thalweg. LCR pile dikes extend 50–150 m (160–500 ft) from shore into the river and have a typical top elevation of 4 m (13 ft) above CRD. Pile dikes are composed of timber piles (0.3-m [1 ft] diameter) spaced 0.8 m (2.6 ft) apart, with a rock apron to prevent toe scour. These structures have 50–60 percent porosity and are intended to decrease flow near the riverbank by redirecting flow toward the thalweg. Due to structural-loading limitations, LCR pile dikes do not extend beyond 10–13 m (33–43 ft) water depth, keeping these structures out of the river thalweg.

The riverbed for much of the main stem LCR is composed of sand, which forms sand waves 1–2 m (3–7 ft) high and 50–100 m (60–330 ft) long. High-flow periods enhance bedload transport, resulting in sand waves 2–4 m (7–13 ft) high. Enhanced sand wave growth during high-flow periods can increase the equivalent roughness height of the river bottom, further increasing river stage.

Effects of Climate Change on Streamflow in the Pacific Northwest

The general circulation models (GCM) in the World Climate Research Programme Coupled Model Intercomparison Project (CMIP) (Taylor and others, 2012) generally indicated in the fourth (CMIP3) and fifth assessment (CMIP5) model ensembles that increased precipitation is likely to occur across Canada and the northern United States, with the largest increases occurring in winter (Climate Impacts Group, 2009), and decreased precipitation is likely to occur in the southern United States, particularly in the summer months (Intergovernmental Panel on Climate Change, 2007). There is, however, a large range among the GCMs in the magnitude of projected changes in precipitation for the Pacific Northwest (Mote and Salathé, 2010; Intergovernmental Panel on Climate Change 2014; Mote and others, 2014).

The effects of changing temperature and precipitation on the hydrologic cycle also have been investigated. Even when considering the uncertainties in future precipitation trends, significant changes in the magnitude and timing of streamflows are a likely outcome of climate change (Groisman and Easterling, 1994; Intergovernmental Panel on Climate Change, 2007). Climate change effects on hydrology have been studied extensively in the Pacific Northwest, including Cayan (1996), Hamlet and Lettenmaier (1999), Stewart and others (2005), and Tohver and others (2014). In these and other studies, a general trend was documented indicating earlier spring peak runoff, less summer runoff, and increased winter streamflows in basins where precipitation in the past has fallen predominantly as snow, but in the future, for transitional (lower elevation) basins, is more likely to fall as rain (Mote and others, 2014; Tohver and others, 2014). Increased winter runoff also implies higher peak flows associated with given recurrence frequencies, which is the basis for the interest in incorporating climate change into design criteria for flood risk reduction levees in Portland. Because higher peak flows are expected in the future, peak-flow statistics derived from the historical period of streamflow record for the Columbia River at The Dalles (14105700; the nearest upstream streamgage on the Columbia River) or the Willamette River at Portland (14211720) or the Willamette River at Newberg (14197900) (the nearest upstream stage gages on the Willamette River) are not adequate for assessing the flood stage on the Columbia corridor levee system.

Previous Climate Change Studies

Future climate hydrographs were developed by first identifying a prototype flood from the historical record, and then projecting that prototype flood into the future to match the statistics of future hydrology. Because the purpose of the study was to investigate an extreme but plausible event, the focus was on one of the more extreme (as in higher temperatures and more precipitation and runoff) future climate scenarios projected by the suite of GCMs available. Previous studies by the USACE and others informed the selection of future climate scenarios.

The Climate Impacts Group (CIG) at the University of Washington has downscaled North Pacific hydroclimate scenarios from the forcing functions generated by six global scale GCMs that were included in the CMIP3 (Hamlet and others, 2013; Climate Impacts Group, 2018). The output of GCMs was statistically downscaled from approximately 50-km^2 to 6-km^2 resolution. The CIG used these downscaled data to provide forcing functions for a hydrologic model (the Variable Infiltration Capacity model; Liang, 1994) that converts meteorological variables such as GCM-derived precipitation, soil moisture, and air temperature into daily values of streamflow. The hydrologic model simulations include three periods of 30 years: 2020s (between 2010 and 2039), 2040s (between 2030 and 2059) and 2080s (2070–99).

Each simulation is additionally identified by the assumption regarding the greenhouse gas emissions scenario that went into the GCM simulation. These scenarios were defined for CMIP3 and described in the Synthesis Report (Intergovernmental Panel on Climate Change, 2007). The most recent climate CMIP5 GCM downscaled streamflow datasets were not available for analysis during this study; however, there were few differences in the two CMIP multimodal ensembles for the Pacific Northwest (Rupp and others, 2013).

For example, the A1B scenario assumes world-wide rapid economic growth and future energy sources to be balanced between fossil intensive and non-fossil sources. The B1 scenario assumes the same world-wide rapid economic growth as in A1B, but with far more reliance on clean and resource-efficient technologies. The A1B scenario is a more extreme scenario of future emissions than the B1 scenario but is moderate compared to the entire range of greenhouse gas emission scenarios defined in Intergovernmental Panel on Climate Change (2000) and those published between 2000 and 2007 (Intergovernmental Panel on Climate Change, 2007; fig. 5, table 1).

The River Management Joint Operating Committee (RMJOC), in collaboration with CIG, assessed the sensitivity of Pacific Northwest hydroclimatology to potential future climate change. The goal of that study was to create hydroclimate streamflow datasets for use by regional planners and water resource modelers (Brekke and others, 2010). On the basis of an initial screening process, the RMJOC selected a subset of the 19 spatially downscaled datasets (each identified by a unique combination of 10 GCMs and 2 CMIP-3 emissions scenarios) that were available from the CIG at the time for further study. The subset was selected to bracket the 10th and 90th percentile of the change in 30-year mean-annual temperature and precipitation, spatially averaged over the entire Columbia-Snake River Basin (Brekke and others, 2010). The scenarios at the extremes of temperature and precipitation change of the selected subset were identified as "more warming and wetter," "less warming and wetter," "more warming and drier," and "less warming and drier." For the purposes of the RMJOC planning study, the entire possible range in climate projections was of interest; for the purposes of this study, only the scenarios at the high end of the range in precipitation and water volume are of interest (fig. 6). The warmer and wetter combination of GCM and emissions scenario selected for this study was the MIROC 3.2 global climate model, and the A1B carbon dioxide emissions scenario, which projects an average temperature increase of about 3 °C for the Columbia Basin in the 2040s, and a basin-aggregated precipitation increase of about 14 percent, compared to the 1971–2000 averages (Brekke and others, 2010). This increase in runoff translates to an annual water year[3] volume of 196 km^3 (159 million acre-ft) at The Dalles, which is an increase of 20 percent over the baseline annual water year volume of 163 km^3 (132.5 million acre-ft; Bonneville Power Administration, 2004). This combination was determined to be the "warmest and wettest" of the 19 downscaled GCM and emissions scenario combinations that were initially screened. It should be noted, however, that only the A1B and B1 emissions scenarios were included in the CIG downscaled datasets, so the selection of the warmest and wettest scenario with respect to the RMJOC study was not necessarily the warmest or wettest climate change projection for the Pacific Northwest derived from the entire suite of CMIP3 models.

[3]The 12-month period from October 1, for any given year, through September 30 of the following year. The water year is designated by the calendar year in which it ends.

Scenarios for greenhouse gas emissions from 2000 to 2100 (in the absence of additional climate policies) and projections of surface temperatures

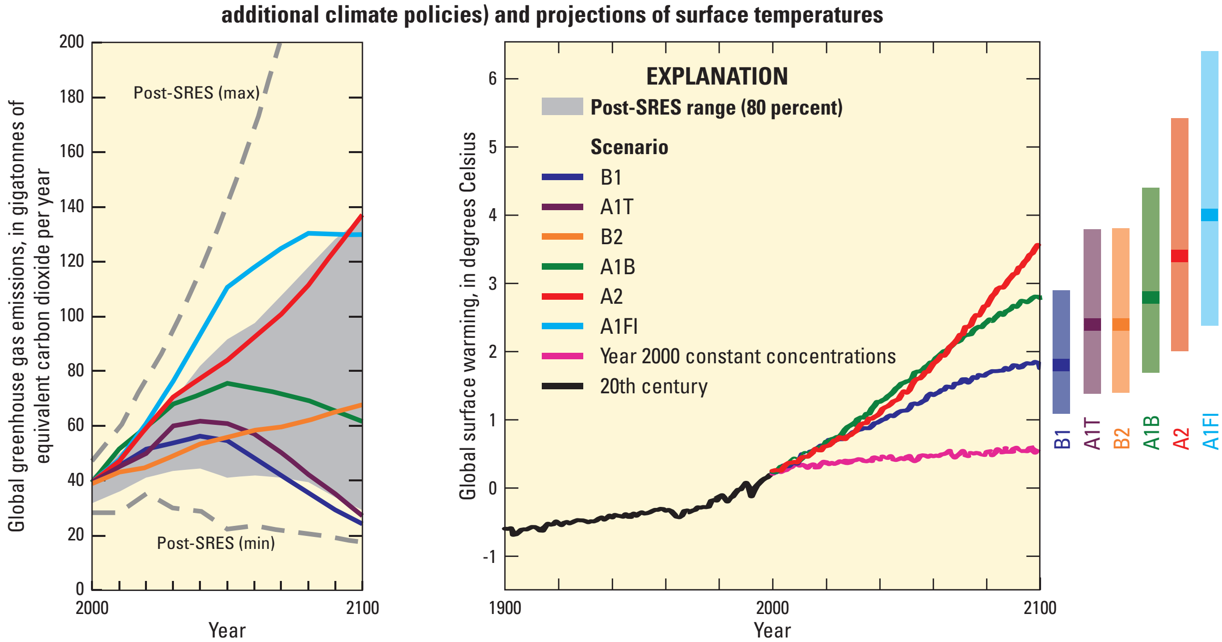

Figure 5. Scenarios for global greenhouse gas emissions and surface warming projections from 2000 to 2100. Definitions of scenarios are shown in table 1; data from SRES (Intergovernmental Panel on Climate Change [2007]).

Table 1. Definitions of greenhouse gas emissions scenarios.

[Source of definitions is Special Report on Emissions Scenarios (Intergovernmental Panel on Climate Change, 2000)]

Scenario family	Development pathway	Scenario	Technological change
A1	Rapid worldwide economic growth, a global population that peaks in mid-century, and rapid introduction of new and more efficient technologies.	A1F1	Fossil intensive energy sources
		A1T	Non-fossil-intensive energy sources
		A1B	Balance between fossil and non-fossil energy sources
B1	Same global population as A1, but with more rapid changes in economic structures toward a service and information economy.		
A2	A very heterogeneous world with high population growth, slow economic development, and slow technological change.		
B2	Intermediate population and economic growth worldwide, emphasizing local solutions to economic, social, and environmental sustainability.		

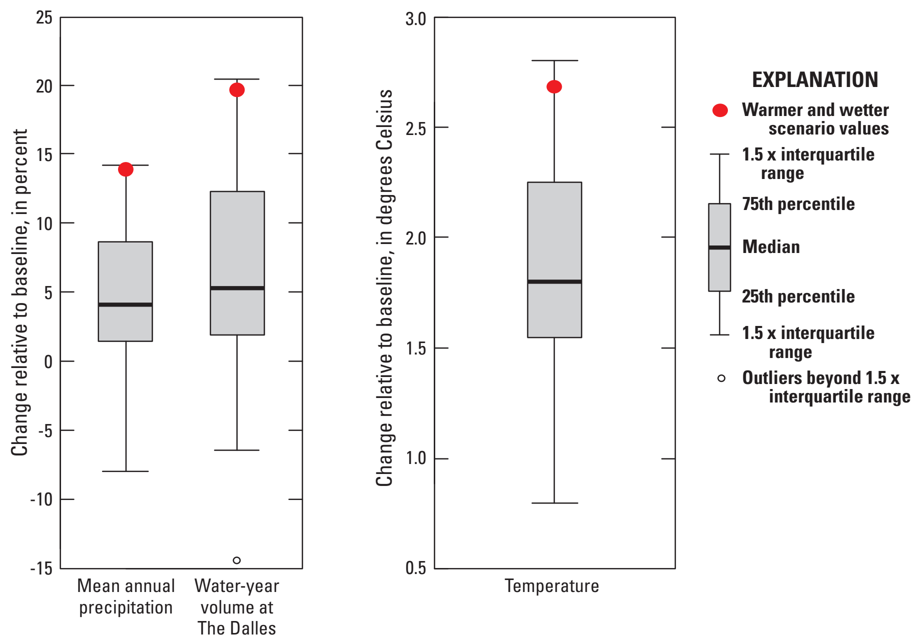

Figure 6. Change in mean annual precipitation and temperature in all future climate scenarios considered by the River Management Joint Operating Committee, and the changes in the warmer and wetter scenario considered in this study.

This study used results of the RMJOC work, which culled a large ensemble of GCMs and emissions scenarios into a regionally appropriate subset and included simulated streamflow data to be used to inform boundary conditions, which was not available for the CMIP5 model ensembles. This smaller selection effectively bracketed the range of possible hydrologic conditions of the ensemble of GCMs. Although the GCMs and emissions scenarios used by the current study may not be the most extreme in terms of wetter or drier, or warmer or cooler conditions, the selection used for the hydraulic modeling does meet the objective of selecting a set of conditions that likely would lead to an extreme but still plausible high-water event.

Selection of Prototype Flood

By using a historical flood as the prototype on which to base future climate hydrographs for an extreme flood, a direct comparison of simulations to observations could be made, and thereby isolate the effects of future climate on the simulated water-surface elevation from flood-specific characteristics such as timing, duration, and total volume. The February 1996 flood was selected as the prototype flood for this study. This flood produced the highest stages at Vancouver, Washington, and Portland, Oregon, in recent history, and was characterized by heavy rain falling on snowpack and frozen ground, and above-average winter Columbia River flow, resulting in high runoff, particularly in the Willamette Valley. The flood was caused by a concentrated inflow of warm and extremely moist air—an atmospheric river—which is expected to become more frequent and intense in the future (Warner and others, 2015). The high Willamette River flows resulting from the warm and heavy precipitation associated with atmospheric rivers, when coupled with moderately high winter Columbia River main stem flows, will be the most likely scenario for extreme high-water stages in the Portland/Vancouver area.

The campaign to construct dams to reduce flood risk on the Columbia River and its tributaries began in response to documented spring floods that devastated population centers in the 19th century. The highest stage of record in the Portland/Vancouver area of about 12.0 m (39 ft) above North American Vertical Datum of 1988 (NAVD 88), was the result of a flood that occurred in June 1894 from snowmelt (U.S. Army Corps of Engineers, 1948). With full Columbia River Basin regulation, a repeat of such a historical snowmelt freshet (typically peaking in May to middle of July) is not likely. Inspection of streamflow since 1970, which is after the Columbia River was regulated, indicates that most annual peak stages at CCLS near Portland occur in the winter (defined as November through March for this study). Roughly two-thirds of all annual peak stages at Vancouver occur during winter (65 percent based on the record from 1998 to 2017 at USGS streamgage 14144700, Columbia River at Vancouver). The extreme high stages near Portland, under current conditions, are caused by the processes represented by a winter storm, which include concurrent high Willamette and Columbia River flows, and Willamette River flows sufficient to cause backwater-induced high stages in the Columbia River at Vancouver just upstream of their confluence. The February 1996 flood, which occurred with full regulation of the Columbia River in place, is just such an event. The peak stage at Columbia River at Vancouver streamgage (14144700) occurred on February 9, at approximately 9.89 m (32.5 ft) NAVD 88 (U.S. Army Corps of Engineers, 1997).

Methods

The LCR is a complex hydro-geomorphic system with natural and built features, where the interaction of tides with fluvial hydraulics produces spatially and temporally variable flow, which results in a temporally variable flow-stage relation throughout the river. To emulate the LCR within the framework of a hydraulic model, many features and processes must be properly simulated by the model to replicate river flow and stage. Relevant terrain features include: coastal bathymetry for the MCR, jetties at the MCR, estuary and riverine bathymetry and topography, pile dikes, levees, and interior flood plain areas (if levees are overtopped), and expression of hydraulic roughness for submerged terrain and features. Relevant hydraulic boundary conditions include ocean astronomical tide phasing and amplitude, non-tidal components of ocean water level, and time-varying river and tributary flow. Successful hydraulic modeling of the LCR is predicated on the ability of a model to properly integrate the terrain features and hydraulic processes and replicate the physics within the focused study area.

The scope for this study focused on evaluating river stage within the fluvial-dominated Lower Columbia River (upstream of RM 38), and specifically for the Portland-Vancouver area (RM 90 to 110; fig. 4). Although salinity and related baroclinic circulation affects the hydraulics of the lower estuary of the Columbia River (RM 0 to 25), salinity effects of the lower estuary have minor influence on river stage within the Portland-Vancouver area, especially during high fluvial discharge periods. For this reason, the study did not include salinity-induced or 3-dimensional circulation effects within the hydrodynamic evaluation. Instead a 2-dimensional approach was used to evaluate LCR hydrodynamics, with the limitation that results may be unreliable downstream of RM 25.

To explore multiple methods of estimating peak stage and understand the uncertainty in simulations, two 2-dimensional hydraulic models of the LCR were developed using Delft3D-Flexible Mesh (Delft3D-FM) and the USACE Adaptive Hydraulics (AdH) frameworks. The models were calibrated to historical high-flows measured in the Willamette River at Portland (14211720) and the Columbia River at Vancouver (14144700) in 1996 and 1997. The 1996 flood produced the highest stage in the Portland area since full regulation was completed in the 1970s, and the high-flow periods in 1996 and 1997 corresponded to the highest recorded daily average flows of 24,500 m^3/s (865,000 ft^3/s) and 19,600 m^3/s (692,000 ft^3/s), respectively, measured at the Columbia River at Port Westward, near Quincy (14246900) from 1991 to 2018. To bracket the uncertainty in Portland vicinity flood stage, the Delft3D-FM model was calibrated to Willamette River stage during the winter 1996 flood that was caused by large Willamette River flows, whereas the AdH model was calibrated to Columbia River stage during the spring 1997 freshet, which was typically caused by high Columbia River flows. The calibrated models then were forced with various extreme but plausible future climate boundaries to simulate potential effects on river stage in the Portland area.

Datasets Used for Hydraulic Models

The data used to build the hydraulic models and validate simulations included stage and discharge data, tidal constituents, high-resolution bathymetry data, maps of levees and log pile dikes, and satellite imagery.

Model Terrain Data

Terrain refers to the topographic and bathymetric data that are required when constructing a model. The USACE obtained lidar topographic data for much of the Columbia River Basin covering an area equal to or greater than the FEMA 0.002 AEP flood plain (Watershed Sciences, 2010). The 1-m lidar data were combined with bathymetric survey data collected in 2010 for the Columbia River and the Willamette River to develop a terrain model with a horizontal resolution of 1 m. For the off-shore bathymetry, the dataset provided by General Bathymetric Chart of the Oceans (GEBCO) was used (General Bathymetric Chart of the Oceans, 2018). It should be noted that parts of the Columbia River Federal Navigation Channel (FNC) were deepened by about 1 m during 2005–10, which is reflected in the lidar data used to generate the model mesh elevations for the simulation years of 1996 and 1997. The deepened terrain used for the model simulations was assumed to have a minimal effect on model performance due to the relatively small affected area.

Aerial Images

Satellite images from Landsat 5 were acquired and compared, when available, to understand inundation on dates with high-flows during the two calibration periods: (1) February 11, 1996, and (2) May 11, 1997 (https://landsatlook.usgs.gov/viewer.html, accessed April 17, 2017). Visual comparison between the images and simulation maps helped to determine if the correct storage areas were being activated during high-flows.

Historical Flood Boundary Conditions

Each hydraulic model has six boundaries requiring data inputs: five upstream river boundaries and one downstream ocean tidal boundary. Hourly hydrographs were applied at the upstream river boundaries, and hourly water-surface elevations were applied at the ocean boundary.

Hourly Flow Hydrographs at the Upstream Boundaries

The five river boundaries include: Columbia River at Bonneville, Willamette River at Willamette Falls, and inflows from the Sandy, Lewis, and Cowlitz Rivers. Washougal River inflow is included by adding one-half its discharge to the Sandy River time series and one-half to the Bonneville time series. Hourly discharge data were applied at the river boundaries for the two historical calibration periods: (1) January 15 to February 28, 1996, and (2) April 12 to July 12, 1997.

Hydraulic model inflow data were obtained from recorded streamflow when possible. The USGS Streamflow Record Extension Facilitator (SREF) computer program (Granato, 2009) was used to fill gaps in the streamflow record and to estimate streamflow outside the period of record or for ungaged sites when streamflow records were incomplete. This program uses the Maintenance Of Variance-Extension, type 1 (MOVE .1) methodology for estimating missing daily-mean streamflow. MOVE.1 produces a regression equation, based on concurrent records between hydrologically similar basins, and then the regression equation coefficients are adjusted to reflect differences in statistics between the concurrent records. After the daily mean streamflow records were extended they were later disaggregated smoothly into hourly or sub-hourly streamflow for model boundary input.

Columbia River at Bonneville Dam—The streamflow input for the Columbia River at Bonneville Dam boundary is a composite of streamflow recorded at The Dalles on the Columbia River (14105700), and tributaries that enter the river between The Dalles and Bonneville Dam, including Klickitat, Hood, White Salmon, Little White Salmon, Wind, Mosier (creek), Eagle (creek) and Kalama Rivers, and includes one-half of the flow measured in the Washougal River (table 2). The Washougal River time series was filled and extended using SREF and recorded data from the East Fork Lewis River streamgage in Washington (14222500).

Sandy River—The streamflow input for the Sandy River boundary was derived by combining recorded data from the Sandy River and one-half of the flow from the SREF-modified Washougal River time series (table 2). The Sandy River streamflow time series was filled and extended using SREF and data recorded farther upstream on the Sandy River near Marmot, Oregon (14137000).

Willamette River at Willamette Falls—The Willamette River boundary is just downstream of the Willamette Falls near Oregon City. The 1996 and 1997 streamflow for this boundary is based on a flow routing procedure used to estimate Willamette River streamflow at the Morrison Bridge (14211720) in Portland, Oregon using recorded data from the Willamette River at Salem (14191000), and the South Yamhill, Pudding, Tualatin, Clackamas Rivers, and Johnson Creek (table 2). The streamflow determined from the flow routing procedure is then applied at the model boundary near the Willamette Falls, circumventing the need to add separate inflow boundaries for all contributing tributaries.

Lewis River—The streamflow input for the Lewis River boundary is a combination of the Lewis and East Fork Lewis Rivers, Washington (table 2). The East Fork Lewis River time series was filled and extended with SREF using recorded data from the Lewis River at Ariel streamgage (14220500).

Cowlitz River—The Cowlitz River boundary corresponds to the confluence and is the combination of the Cowlitz and Coweeman Rivers, which are both gaged. The SREF software was used to fill and extend the Cowlitz River time series using upstream data, and the Coweeman River time series was similarly modified using data from the Toutle River (table 2).

Table 2. Sources and types of data from measurement sites in the Columbia and Willamette River Basins, Oregon and Washington.

[Locations of sites are shown in figure 1. **Managing agency:** NOAA, National Oceanic and Atmospheric Agency; NWS, National Weather Service; USGS, U.S. Geological Survey. **Abbreviations:** OR, Oregon; NA, not applicable; WA, Washington]

Boundary	Data type	Contributing sites	Adjustments and factors	Site No.	Managing agency
Columbia River at Bonneville Dam	Streamflow	Columbia River at The Dalles, OR	NA	14105700	USGS
		Klickitat River near Pitt, WA	NA	14113000	USGS
		Hood River at Tucker Bridge, near Hood River, OR	NA	14120000	USGS
		White Salmon River near Underwood, WA	NA	14123500	USGS
		Little White Salmon River near Cook, WA	NA	14125500	USGS
		Wind River near Carson, WA	NA	14128500	USGS
		Mosier Creek near Mosier, OR	NA	14113200	USGS
		Washougal River near Washougal, WA	0.5 times flow	14143500	USGS
		Lewis River at Ariel, WA	MOVE.1 to fill/extend 14143500	14220500	USGS
Sandy River	Streamflow	Sandy River below Bull Run River, OR	NA	14142500	USGS
		Sandy River near Marmot, OR	MOVE.1 factor 1.15 to fill/extend 14142500	14137000	USGS
		Washougal River near Washougal, WA	0.5 times flow	14143500	USGS
		Lewis River at Ariel, WA	MOVE.1 to fill/extend 14143500	14220500	USGS
Willamette River at Willamette Falls	Streamflow	Willamette River at Salem, OR	NA	14191000	USGS
		South Yamhill River at McMinnville, OR	NA	14194150	USGS
		Willamette River at Newberg, OR	NA	14197900	USGS
		Pudding River at Aurora, OR	NA	14202000	USGS
		Tualatin River at West Linn, OR	NA	14207500	USGS
		Clackamas River at Estacada, OR	NA	14210000	USGS
		Johnson Creek at Milwaukie, OR	NA	14211550	USGS
Lewis River	Streamflow	East Fork Lewis near Heisson, WA	MOVE.1 factor 1.94 to fill/extend 14143500	14222500	USGS
		Lewis River at Ariel, WA	MOVE.1 factor 1.70 to fill/extend 14222500	14220500	USGS

Table 2. Sources and types of data from measurement sites in the Columbia and Willamette River Basins, Oregon and Washington.—Continued

Boundary	Data type	Contributing sites	Adjustments and factors	Site No.	Managing agency
Cowlitz River	Streamflow	Cowlitz River at Castle Rock, WA	NA	14243000	USGS
		Cowlitz River below Mayfield Dam, WA	MOVE.1 to fill/extend 14243000	14238000	USGS
		Coweeman River near Kelso, WA	NA	14245000	USGS
		South Fork Toutle River at Toutle, WA	MOVE.1 to fill/extend 14245000	14241500	USGS
		Toutle River at Tower Road near Silver Lake, WA	MOVE.1 to fill/extend 14245000	14242580	USGS
Validation data					
River	**Data type**	**Site name**	**Purpose**	**Site No.**	**Managing agency**
NA	Stage	Toke Point, WA	Evaluate storm surge from non-tidal residual	9440910	NOAA
Columbia River	Streamflow	Columbia River at Port Westward near Quincy, OR	Evaluate annual peak flow statistics	14246900	USGS
Columbia River estuary	Stage	Astoria/Tongue Point, OR	Validate simulated stage	9439040	NOAA
Willamette River	Stage	Willamette River at Portland, OR	Validate simulated stage	14211720	USGS
Columbia River	Stage	Columbia River at Vancouver, WA	Validate simulated stage	14144700	Historical: NWS Current: USGS
Columbia River	Stage	Columbia River below Bonneville Dam, OR	Validate simulated stage	14128870	USGS

Water-Surface Elevations Offshore of the Mouth of the Columbia River

Water levels recorded by the National Oceanic and Atmospheric Administration (NOAA) at Astoria, Oregon (9439040) were used to determine the ocean boundary conditions, which was accomplished differently in the two models. The methods used for each model are described in section, “Two-Dimensional River Stage Modeling.”

Historical Events Calibration Data

Both models were calibrated to water levels at three sites within the model reach. Water levels recorded at the NOAA stage gage at Astoria were used for calibrating to tidal elevations in the lower estuary. Water levels recorded on the Willamette River at Portland (USGS 14211720) and on the Columbia River at Vancouver (USGS 14144700) were used to establish a good calibration to the fluvially dominated river stage near Portland.

Future Climate Boundary Conditions

Boundary conditions representing extreme but plausible future conditions were developed in the form of hydrographs at the upstream inflow boundaries and water-surface elevation time series at the ocean boundary. The development of those future boundary conditions for a high-flow event was patterned on the February 1996 winter storm.

Hydrology and Streamflows

Several steps were required to convert the results from a GCM to streamflow at the locations represented by the models’ upstream boundaries. First, future runoff was simulated with the Variable Infiltration Capacity hydrologic model, using downscaled meteorological boundary conditions as simulated by the MIROC 3.2 GCM assuming an aggressive carbon dioxide emissions scenario (SRES A1) for 2030–59. This step was done by the Climate Impacts Group at the University of Washington, and the datasets produced are available for download (Climate Impacts Group, 2018).

Using this Variable Infiltration Capacity-simulated runoff, a future unregulated 2040s streamflow at Bonneville Dam on the Columbia River and Willamette Falls on the Willamette River was simulated. This was done by running the USACE Hydrologic Engineering Center (HEC) Reservoir System Simulation software for the Columbia River Basin through the 2040s to simulate natural conditions within the basin, but assuming that downstream dams had not yet been constructed.

Because a direct comparison of statistics between historical streamflows and future streamflows was required, historical streamflows were converted to an unregulated condition to match the unregulated condition of the future streamflows. This was done by running the Reservoir System Simulation software through water years 1928–98, again simulating the effect of large natural lakes before dams had been constructed.

The HEC Statistical Software Package, version 2.1, was used to generate peak annual winter (November–March) unregulated flow rankings for the historical and future datasets. The resulting estimated flow ranges and rankings were based on the unregulated datasets of 1928–98 and 2030–59 for the historical and future periods, respectively, which enabled ranking of peak winter flows (table 3). Comparing the rankings of historical, winter, unregulated peak-flow periods to future, winter, unregulated peak-flow periods provided scaling factors that were applied to historical period hydrographs to create extreme but plausible future condition hydrographs.

Table 3. Peak-flow rankings for historical winter unregulated flow and future winter unregulated flow, Columbia and Willamette Rivers, Oregon, winter 1996.

[Flows based on Bulletin 17B flood-frequency analysis (Interagency Advisory Committee on Water Data [1981]) using the U.S. Army Corps of Engineers Hydrologic Engineering Cener statistical software package. Flows are in thousands of cubic meters per second (1,000 m^3/s) and thousands of cubic feet per second (1,000 ft^3/s)]

Rank of low to high probability	Historical unregulated flow		Future unregulated flow (2040s)		Difference (percent)
	(1,000 m^3/s)	(1,000 ft^3/s)	(1,000 m^3/s)	(1,000 ft^3/s)	
Columbia River at Bonneville Dam					
1	15.89	561	21.38	755	34.6
2	14.05	496	19.77	698	40.8
3	12.69	448	18.49	653	45.8
4	11.35	401	17.16	606	51.0
5	9.66	341	15.26	539	58.3
6	8.35	295	13.71	484	64.1
7	7.02	248	11.98	423	70.3
8	5.07	179	9.06	320	78.7
9	3.68	130	6.71	237	82.1
10	3.14	111	5.69	201	81.7
11	2.74	96.8	4.93	174	80.2
12	2.14	75.5	3.74	132	74.8
Willamette River below Willamette Falls					
1	12.23	432	14.98	529	22.3
2	10.96	387	13.82	488	26.2
3	9.99	353	12.88	455	29.1
4	9.03	319	11.92	421	32.0
5	7.73	273	10.50	371	35.8
6	6.74	238	9.32	329	38.6
7	5.69	201	8.01	283	40.9
8	4.08	144	5.80	205	42.4
9	2.89	102	4.02	142	39.4
10	2.40	84.9	3.28	116	36.1
11	2.06	72.9	2.73	96.6	32.5
12	1.54	54.4	1.91	67.4	23.9

The historical hydrograph, representing an extreme high-flow, was the 0.005 AEP flood that occurred in winter 1996. The USACE computed an unregulated peak flow of approximately 14,100 m^3/s (500,000 ft^3/s) for this flood on the Columbia River at The Dalles (14105700; U.S. Army Corps of Engineers, 1997) and interpolation between the first and second ranked peak flows indicated that the corresponding future peak flow was approximately 40 percent greater (table 3). Similarly, the computed historical peak flow at Willamette River below Willamette Falls in winter 1996 was 12,200 m^3/s (432,000 ft^3/s) (U.S. Army Corps of Engineers, 1997), about 20 percent less than the corresponding future unregulated peak flow for the same ranking (table 3). Therefore, the 1996 historical hydrographs at the inflow boundary locations were perturbed to a 2040's level by applying a scaling factor of 1.4 and 1.2 at Bonneville Dam on the Columbia River and the Willamette River below Willamette Falls, respectively (fig. 7). Future flood hydrographs for the lower Columbia River tributaries—Washougal, Sandy, Lewis, and Cowlitz Rivers—were determined by using a scaling factor of 1.2 to correspond with the Willamette River, because insufficient data were available for the smaller lower Columbia River tributary basins to make river-specific scale factor estimates. For modeling purposes, these basins were scaled with the same factor as the Willamette River Basin because it seemed likely they would respond similarly to future atmospheric river events. These perturbed hydrographs were used as the inflow hydrographs in the future conditions hydraulic simulations.

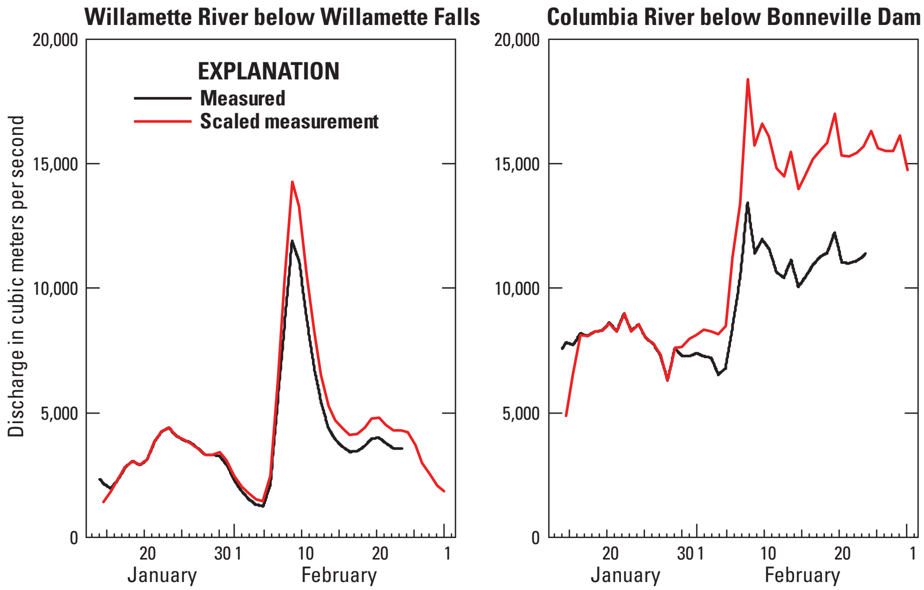

Figure 7. Future inflow flood hydrographs for the Columbia River at Bonneville Dam and the Willamette River below Willamette Falls, Oregon.

Water-Surface Elevations Offshore of the Mouth of the Columbia River

The water-surface elevation imposed at the Pacific Ocean Boundary comprises three parts: (1) mean sea level, (2) storm surge deviations from mean sea level, and (3) deviations from mean sea level because of astronomical tides.

Mean Sea Level—The projections of future changes in mean sea level (MSL) depend on the assumptions made about greenhouse gas emissions in the future, the rate of warming of the climate, and future rate of terrestrial ice-sheet melting and collapse. At a given coastal location, relative changes in local MSL reflect the integrated effects of global MSL change plus changes of regional geologic, oceanographic, or atmospheric origin. The locally affected potential for future sea level is referred to as relative SLC and its effects should be considered as far inland as the extent of estimated tidal influence. In this study, a range of SLC realizations was considered because it is problematic to assign a specific value to future SLC (Hinkel and others, 2015).

The scenario-based approach bounds the range of potential SLC realizations using three equally plausible scenarios: low, intermediate, and high. Each of the three USACE scenarios is based on the latest science from Intergovernmental Panel on Climate Change (IPCC), NOAA and National Research Council (NRC) and is specific to individual NOAA tide stations (U.S. Army Corps of Engineers, 2018). The three SLC scenarios applicable for Astoria, Oregon (NOAA stage-measurement site 9439040) are shown in figure 8. In this study, three values for SLC were used that provided a wide range over which to evaluate the sensitivity of flood stage at Portland to a climate change-affected ocean boundary. These three values can be placed into the context of the USACE scenarios as follows:

1. SLC 0 m: The USACE low scenario for future SLC is an extrapolation from the measured historical rate derived from NOAA tide gages. For 2040, the USACE projection for Astoria is -0.015 m (due to local tectonic uplift of the coast) using a base year of 1992, so the lowest value of SLC considered in this study was 0, representing no change from baseline conditions.

2. SLC 0.25 m: The USACE “intermediate” future SLC scenario accounts for the thermal expansion of the oceans and loss of ice from Antarctica and Greenland. The SLC of 0.25 m corresponds to a high USACE scenario in 2040 or an intermediate USACE scenario in 2094.

3. SLC 1 m: To provide a context for assessing how an accelerating SLC in years beyond 2040 might affect the results shown, a third value of 1.0 m SLC was simulated. This value corresponds to the USACE “high” scenario in the year 2088.

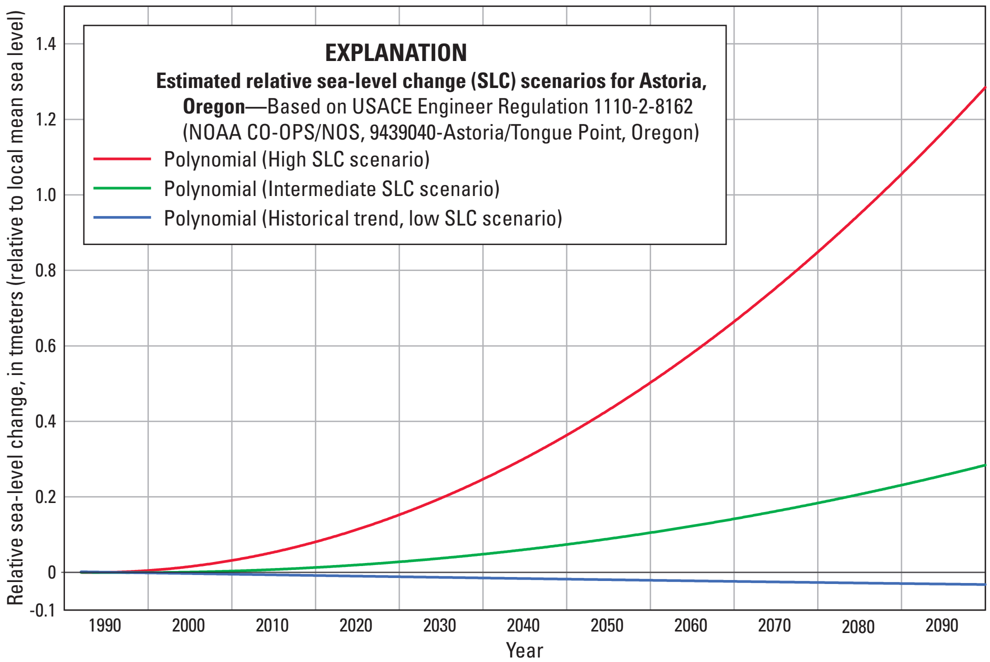

Figure 8. Estimated sea-level change scenarios at Astoria, Oregon. Projections based on U.S. Army Corps of Engineers (2018).

Non-Tidal Residual Associated with Maritime Storms—Based on its close proximity to the coastal ocean, the NOAA tide gage at Toke Point, Washington (9440910; fig. 1) was used to define the non-tidal residual due to maritime storms affecting the region of northwest Oregon and southwest Washington coast. The Toke Point tide gage is located at the mouth of Willapa Bay 8 km from the open coast and 50 km north of the MCR. The Willapa Bay inlet has not been altered, and remains as a broad unobstructed tidal interchange from estuary to ocean. Because of this, the storm-induced non-tidal residual (storm surge) signal observed at Toke Point is unaltered, unlike tidal gages that are located within estuaries like the LCR where the inlet has been engineered/confined. Storm surge (non-tidal residual) was determined by subtracting the astronomical tide reconstructed from tidal harmonics at Toke Point from the total water level recorded at Toke Point. Based on these considerations, storm surge computed for Toke Point is assumed to be a close approximation for open coast storm surge applicable for the coastal realm of the MCR.

The 0.5 AEP non-tidal residual associated with storm surge at Toke Point is 1.05 m (3.4 ft), based on a 43-year period of record. Non-tidal residual during storms frequently exceeds 0.6 m (2.0 ft), during average annual conditions. Three significant storms were identified, with peak water levels between 1.4 and 1.6 m (4.6 and 5.2 ft; fig. 9). The highest and broadest peak of non-tidal residuals associated with storm surge occurred in December 2007, with peak levels greater than 1.4 m that persisted for 14 hours. Therefore, the storm surge of December 2–6, 2007, was used as the prototype for the storm surge in future climate simulations. The calculated storm surge at Toke Point was scaled by a factor of 0.91 to convert the storm surge at Toke Point from an AEP recurrence of 0.02 to 0.05. This reduction in AEP intensity was implemented to develop a plausible total water level and to avoid imposing an excessively extreme ocean boundary condition of maximum spring tide sequence combined with maximum storm-induced non-tidal residual. The resulting time series of storm surge was added to the mean sea level projection and to the reconstructed tides (see section, “Astronomical Tidal Signal”).

Astronomical Tidal Signal—Tidal estimates at the location of the Astoria stage gage (9439040) were used to develop the astronomical tidal component of the future climate ocean boundary condition. In this study, no changes to sedimentation or accretion that might affect the tidal signal at the MCR were assumed. These “estimates” are reconstructions of the tides from the component tidal harmonics, the amplitude and phases of which are determined for individual locations based on the historical record of tides measured at that location. These estimates remove the non-tidal effects that are embedded in the records and can be compiled and downloaded

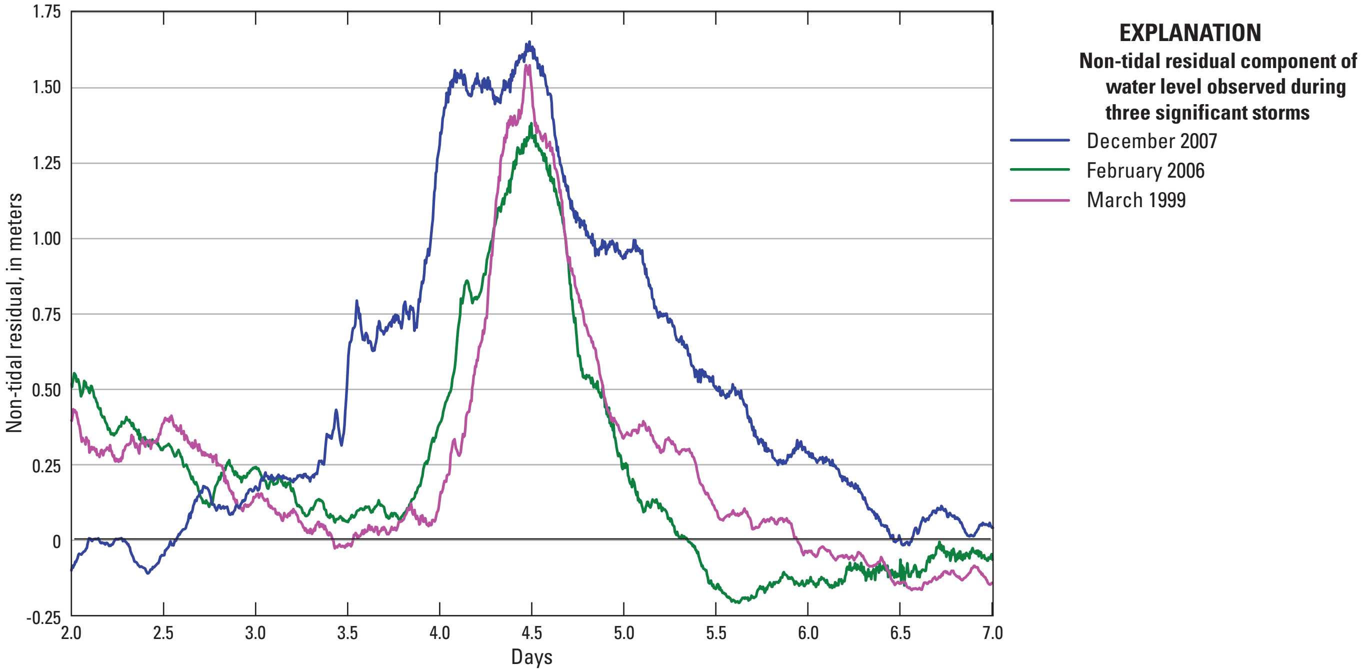

Figure 9. Storm surge peak water levels at Toke Point, Washington, March 1999, February 2006, and December 2007. Non-tidal residual component of water levels based on tidal gage at Toke Point (NOAA 9440910) for a 45-year period of record. The time series were aligned so the maximum value for each is coincident (at 4.5 days) to enable a unified comparison of each time series.

from the NOAA website: https://tidesandcurrents.noaa.gov/tide_predictions.html. For the purpose of this study, tidal estimates at the Astoria stage gage through 11 water years (October 1, 1995—September 30, 2006) were analyzed. The 5-day running mean of the daily maximum tidal water level was computed. The maximum of this 5-day running mean, during the 11 water years considered, occurred on February 9, 2003. The time series of predicted tide centered on this date was used as the prototype for the astronomical tide in the future climate simulations by centering the high tide that occurred February 9, 2003, at 26 days and 12 hours in the future climate simulations and centering the peak in the time series of the non-tidal residual representing storm surge at 26 days and 0 hours, which aligned semi-diurnal tidal peaks with the maximum in the storm surge (table 4; fig. 10).

Two-Dimensional River Stage Modeling

The approach of this study was to use two independently developed 2-dimensional hydraulic models to simulate water-surface elevation in the LCR and compare the output of the two models as an additional constraint on the precision of the results. The first model uses the Delft3D-Flexible Mesh (FM) platform; the second model uses the USACE Adaptive Hydraulics (AdH) platform. Both models were calibrated and

Table 4. Timeline of peak stage and discharge in future climate prototype flood along the Columbia and Willamette Rivers, Oregon and Washington.

Event description	Day	Hour
Start of simulation	0	0
Maximum discharge at Bonneville on the Columbia River	24	0
Maximum discharge at Willamette Falls on the Willamette River, Oregon	25	0
Higher high water at Astoria, Oregon	25	12
Maximum stage at Vancouver, Washington	25	18
Maximum stage at Portland, Oregon	25	18.5
Maximum peak in storm surge at Astoria, Oregon	26	0
Lower high water at Astoria, Oregon	26	1
Higher high water at Astoria, Oregon	26	12
End of simulation	44	0

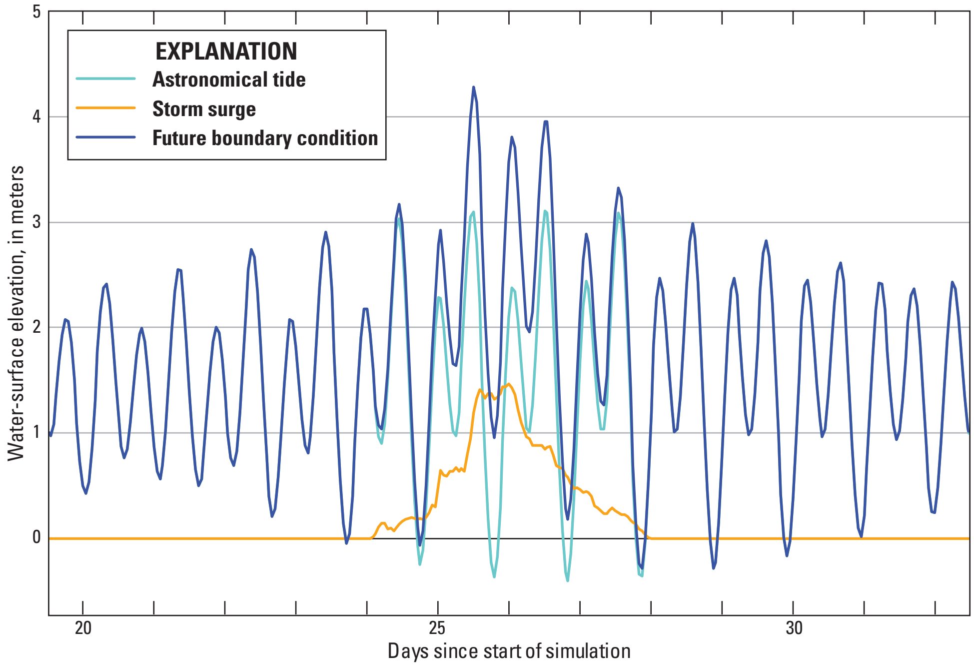

Figure 10. Simulated astronomical tide, storm surge, and future tidal conditions at the mouth of the Columbia River, Oregon and Washington.

validated with historical flows and historical sea level during high-flows occurring during January and February 1996 and April through July 1997. Both models then were used to simulate an extreme but plausible future climate scenario based on the February 1996 period, while considering three values for SLC at the MCR, resulting in three future climate simulations from each model. Important aspects of both models include the progression of LCR model development, model-specific aspects of how the ocean boundaries are handled, and the different way physical structures are embedded into the model mesh.

Hydraulic Model Comparison

This study compared the simulated outputs of the two models that were individually calibrated but used similar geometries, parameters, and boundary conditions. The domain of the LCR in both models extends from the Bonneville Dam on the Columbia River and the Willamette Falls, to 30–40 km offshore into the Pacific Ocean (fig. 1).

The models differed in their mesh resolution and the approach of representing physical structures. The Delft3D-FM model was coarser (fig. 11*A*), with 26,086 nodes and 39,382 flow elements, than the AdH mesh, which included about 268,000 nodes and about 518,000 elements (fig. 11*B*). For the Delft3D-FM model, the weir tool was used to draw the levee and pile dike features onto the model mesh and assign top elevations (figs. 12*A* and *B*). Alternatively, the AdH model, with its fine mesh, was able to resolve levees and represent nominal spatial attributes of pile dikes within the mesh and then assign appropriate heights, Manning’s n roughness coefficients, and vegetation classes to those mesh cells (figs. 12*C* and *D*). Additionally, the two models used different friction formulations, with Delft3D-FM using the Chézy formula and roughness coefficients, and AdH using the Manning formula and Manning’s n values (table 5).

Despite these differences, many model specifics were the same. The number, location, and height of levees included in the models were the same in size and crest elevation. Levee elevations were assigned based on lidar and as-built surveys (table 6). The two models also used the same terrain data, a composite of lidar and bathymetric surveys compiled in 2010 (described in section, “Model Terrain Data,”) to assign ground elevation to mesh cells. Lastly, the riverine boundary conditions were developed from the same hydrographs, with the Delft3D-FM model applying discharge values at an hourly time step and the AdH model applying discharge values at a daily time step.

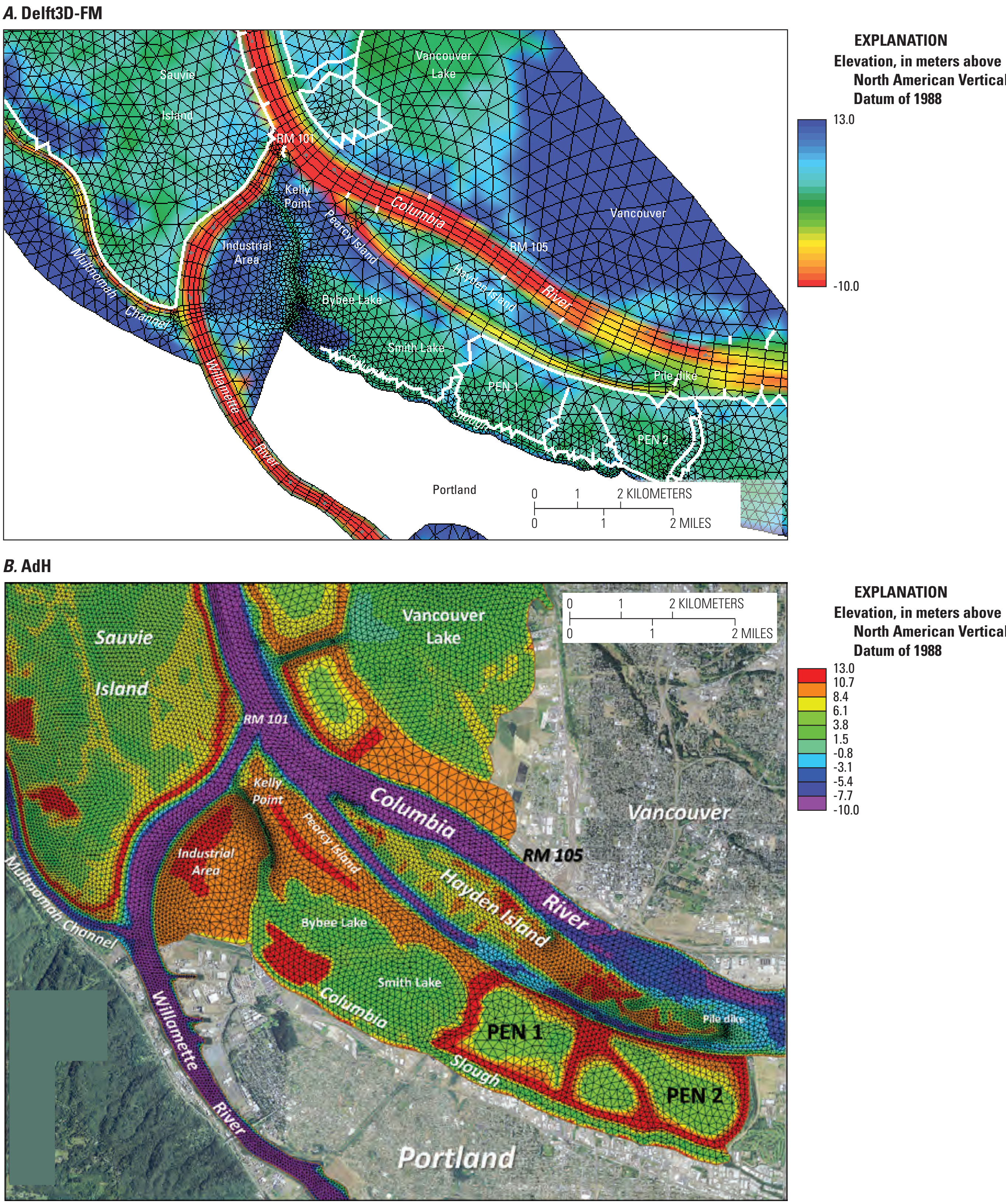

Base from U.S. Army Corps of Engineers

Figure 11. Comparison of Delft3D-Flexible Mesh (Delft3D-FM) (*A*) and Adaptive Hydraulics (AdH) (*B*) model meshes with assignments of elevation along the Columbia and Willamette Rivers, Oregon.

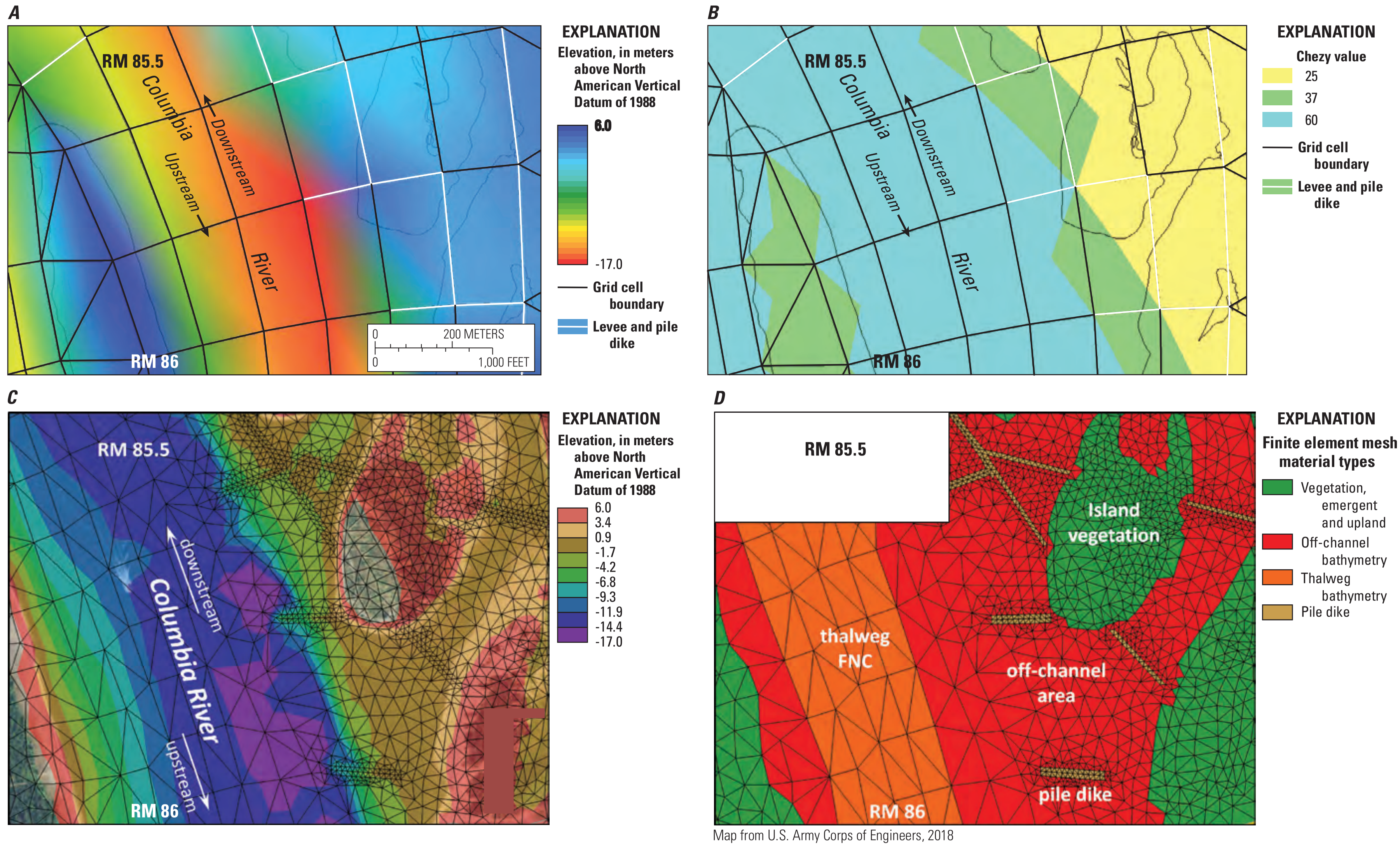

Figure 12. Comparison of Delft3D-Flexible Mesh (Delft3D-FM) mesh with assignments of bathymetry (*A*) and roughness coefficients (*B*), to Adaptive Hydraulics (AdH) mesh with assignments of bathymetry (*C*) and mesh material types (*D*) along the Columbia and Willamette Rivers, Oregon.

Table 5. Model roughness values for Delft3D-Flexible Mesh (Delft3D-FM) and Adaptive Hydraulics (AdH) along the Columbia and Willamette Rivers, Oregon.

[–, no data]

Model domain	Friction coefficient value	
	Delft3D-FM Chézy	AdH Manning's n
Ocean	86	0.015
Estuary		
Main channel	54–86	0.015
Tidal flood plain	5–56	0.025
Above estuary		
Main channel	37–56	0.0265
Secondary channel	25	0.0275
Flood plain	5–25	0.05
Channel island	5	0.08
Jetty/pile dike	–	0.05–0.08

Table 6. Elevation data compiled from light detection and radar surveys along the Columbia corridor levee system, Oregon and Washington.

[Values determined from U.S. Army Corps of Engineers lidar dataset. River miles shown in figures 2–4. **Abbreviations:** ft, foot; m, meter; MCDD, Multnomah County Drainage District #1; RM, river mile; NAVD 88, North American Vertical Datum of 1988; NA, not applicable]

Levee name	Diking district	Columbia River (RM)	Top of levee crest elevation above NAVD 88			
			Upstream		Downstream	
			(m)	(ft)	(m)	(ft)
Skamokawa/Price Island	Wakiakum 4	34.2–38.9	4.8	15.7	4.8	15.7
Tenasillahe Island	Clatsop 6 (inactive)	34.8–36.5	4.3	14.1	5.0	16.4
Puget Island/Little Island	Wakiakum	39–46	5.1	16.7	4.7	15.4
Web, Westland, Woodson	NA	44.5–49	5.5	18.0	5.2	17.0
Midland	NA	49–50	5.5	18.0	5.5	18.0
Cowlitz 15	NA	57–59	6.6	21.7	6.6	21.7
Deer Island	NA	77–82.5	9.8	32.2	9.7	31.8
Woodland	Cowlitz 2	81.25–86	11.5	37.6	9.2	30.2
Lake River Delta	NA	88–90	8.5	27.8	8.5	27.8
Bachelor Island - North	NA	89–90.5	8.5	27.8	6.0	20.0
Bachelor Island - South	NA	88.5–90	7.7	25.3	7.7	25.3
Scappoose	NA	90–99.25	10.7	35.1	10.3	33.8
Clark County DD 14 - North	Ridgefield	94–95.5	8.5	27.9	8.0	26.3
Clark County DD 14 - South	Ridgefield	95.5–102.5	9.1	29.8	8.1	26.3
Sauvie Island	Columbia 1 (inactive)	93–98	9.0	29.5	9.0	29.5
Sauvie Island	Sauvie Diking District	98.3–101.5	10.9	35.8	10.9	35.8
Peninsula 1	MCDD	105.5–106.5	11.7	38.4	11.1	36.4
Peninsula 2	MCDD	106.5–108.5	11.6	38.1	11.5	37.7
Multnomah County - West	NA	108.5–115	13.0	42.0	12.5	41.0
Multnomah County - East	NA	115–118.5	13.7	44.0	13.0	42.0
Sandy Diking District	NA	118.5–123	14.5	46.0	13.7	44.0
Steigerwald	NA	123.9–128	14.1	46.3	13.1	42.9

Delft3D-Flexible Mesh

The Delft3D-FM Suite is an open-source hydrodynamic model, capable of calculating combinations of 1D, 2D, and 3D unsteady flow over unstructured meshes in riverine and estuarine systems. It was developed by Deltares in the Netherlands, a research institute with a long history of hydrodynamical simulation throughout the world (Deltares, 2015). Delft3D-FM is the successor to the structured Delft3D Suite which was developed in the late 1980s. The unstructured mesh used in Delft3D-FM pairs rectangular, curvilinear cells, for main channel flow, with triangular cells for off-channel flow. This approach provides greater flexibility than structured meshes in adapting the resolution of the mesh to the underlying bathymetric and topographic gradients, and in aligning mesh boundaries to complex, difficult-to-follow boundaries on the ground. Delft3D-FM then solves the unsteady shallow water equations using the finite volume method on the unstructured mesh.

Delft3D-FM solves the Navier-Stokes equations for an incompressible fluid in two dimensions by depth averaging, which is the approach used in this study, and under the shallow water and Boussinesq assumptions. Under these assumptions, the vertical momentum equation is reduced to the hydrostatic pressure equation and vertical accelerations due to buoyancy effects and changes in topography are not considered. Because of mesh coarseness, the Navier-Stokes equations were Reynolds averaged to describe turbulent flow at the mesh scale; this process introduces Reynolds stresses. A k-epsilon turbulence closure model was then used to relate the Reynolds stresses to the Reynolds-averaged flow quantities. The equations are formulated in orthogonal curvilinear coordinates and the free surface level and bathymetry are related to a flat horizontal plane of reference, which, in this study, was the North American Vertical Datum of 1988 (NAVD 88).

Lower Columbia River Model Development

In 2012, the USGS Coastal and Marine Geology Program and Deltares collaborated to develop a coupled Delft3D-Simulating Waves Nearshore structured model system, including hydrodynamic, wave, and sediment transport components, for the mouth of the Columbia River with the purpose of state-of-the-art simulation of sediment transport in the dynamic estuary entrance (Elias and others, 2012). Continuing with this research collaboration, a second study was developed to explore the effect of discharge on tidal hydrodynamics for a range of discharge classes (Van der Steeg, 2016). In the second study, the modeling suite was updated to the unstructured Delft3D-FM system and the study domain was expanded to include the entire LCR.

The first iteration Delft3D-FM LCR model developed in Van der Steeg (2016) extends from the Columbia River at Bonneville Dam and Willamette River at Willamette Falls in Oregon City to about 137 km offshore from the MCR into the Pacific Ocean. The large model domain allowed simulation of ocean tide propagation into the Columbia River estuary and LCR, replication of fluvial flow from LCR main stem and tributaries, and tides interacting with riverine flow. The initial model domain had spatial resolution that varied from 100 to 2000 m, and was represented by approximately 25,375 nodes. Nodal point elevations within the Delft3D-FM model mesh were interpolated from the 2010 Lower Columbia Terrain Model developed from lidar and multibeam bathymetric survey data by the USACE Portland District in support of the Columbia River Treaty. With its focus on the estuary and effects of discharge and tides, this Delft3D-FM LCR model was fully 3-dimensional and accounted for salinity propagation.

Lower Columbia River Model for Climate Change Study

Prior to this study, the Delft3D models developed by USGS Coastal and Marine Geology Program were focused studies of the LCR estuary, which did not require the same level of upstream flood plain coverage in the model mesh that was required for this study. Because this study explored the effects of extreme but plausible high flows on the Columbia Corridor Levee System, it was critical to include flood plains in the LCR that might be inundated during high flow. Greater detail was added to Van der Steeg's (2016) first-iteration unstructured mesh to include more LCR flood plain, and inflow was added from appropriate tributaries. Mesh and model modification tasks were required to create a Delft3D-FM model that would be appropriate to use for this Levee Ready Columbia (LRC) study:

1. Increase the mesh coverage to include relevant flood plain with the potential for inundation during peak flow conditions, specifically around North Portland peninsula, Multnomah Channel, and the Columbia River slough.

2. Expand mesh coverage to include interior areas behind levees, specifically the North Portland peninsula and Sauvie Island, to model the effect of interior area storage (and hydrograph effects) should the levees become overtopped.

3. Expand the mesh to include inflow from relevant tributaries, specifically the Sandy, Lewis, and Cowlitz Rivers. The lowest 1–2 km of these tributaries was incorporated into the model mesh in order to accurately convey the inflows into the main river channel.

4. Include weir structures to portray levees and pile dikes with appropriate crest elevations.

When the enhancements to the model mesh were complete, it was composed of 39,382 elements, 26,086 nodes, 122 weir structures to represent off-channel levees, and 137 weir structures to represent in-channel pile dikes.

Physical Parameters—Flow characteristics were assigned to the mesh cells using triangulation from values specified at discrete point locations. Each cell was assigned an average elevation value (figs. 12*A* and 12*C*) based on high-resolution bathymetry data provided by the USACE and GEBCO. Chézy roughness values also were mapped onto the mesh using Helaire (2016) and Elias and others (2012) initially and refined to optimize calibration to the historical events. Generally, Chézy values were 86 in the ocean, ranged from 54 to 86 in the estuary, were 50 along the main channel and flow paths, and were 5 to 25 over vegetated flood plain areas (table 5; figs. 12*B* and 12*D*).

Hydraulic Structures—The last step of model construction was to map flow structures, such as pile dikes and levees, that were not fully captured at the mesh resolution. In Delft3D-FM, the “weir” tool was used to represent these features and their maximum height information in the model. Pile dike locations were determined using maps and aerial images (Google Earth) and represented by weirs at the nearest cell edges in the model (white lines in figures 12*A* and 12*B*). The Delft3D-FM weir structure was used to simulate levees throughout the lower Columbia River. Levees were placed at their correct locations, crest, and height with maps and lidar data (U.S. Army Corps of Engineers, 2010).

Boundary Conditions—Boundary conditions for river inflow are applied in the model at each of the five upstream tributary locations using a time-varying flow boundary condition at a 1-hour time step. Inflow boundary conditions used USGS data for the Columbia River at Bonneville Dam, Sandy River, Washougal River, Willamette River, Lewis River, and Cowlitz River as described in section, “Hourly Flow Hydrographs at the Upstream Boundaries.” The head of tides for the Washougal River was not implemented in the Delft3D-FM model, because the tributary flow from this drainage was not deemed relevant in comparison to the other four tributaries. Instead, flow from the Washougal River was split and applied to the Sandy River and Bonneville Dam inflows.

The offshore area of the MCR in the Delft-FM model domain is roughly rectangular, about 54 km in latitude and 42 km in longitude (fig. 1). The ocean boundary condition was a specified water elevation at the upper and lower left corners of this rectangle (fig. 1) in several steps. First, the amplitude and phase of 13 tidal constituents (M2, S2, N2, K2, K1, O1, P1, Q1, Mf, Mm, M4, MS4, and MN4; Talley and others, 2011) were determined at the location of the upper and lower left corners of the ocean boundary using tidal prediction software developed by Oregon State University (Egbert and Erofeeva, 2002). The model was run through the period of the 1996 and 1997 historical floods with these tidal constituents specified as boundary conditions (amplitude and phase) at the upper and lower left corners of the ocean boundary. The amplitude and phase of the same 13 tidal constituents were extracted from the simulated time series at Astoria using the ftide function of the TideHarmonics package in R version 3.3.2 (R Core Team, 2016; Stephenson, 2016). The simulated amplitudes and phases were compared with the published amplitudes and phases of the tidal constituents at Astoria (https://tidesandcurrents.noaa.gov/harcon.html?id=9439040, accessed February 28, 2017) to calculate a correction to the amplitude and phase at the boundary locations. The model was run again with these corrections, and the simulated time series at Astoria was again compared to the recorded elevation. This time, the comparison was done by subtracting the recorded time series from the simulated time series to obtain a non-tidal residual, and then smoothing that residual with a 5-day moving average. The smoothed residual was added into the hourly tidal time series at the upper and lower left corners of the ocean boundary to provide the next iteration of the ocean boundary condition. The model was run again, and a 3-day moving average of the residual at Astoria was calculated and added into the boundary conditions time series to provide the final ocean boundary condition.

To obtain ocean boundary conditions for the future climate simulations, the model simulated the historically high tide period from November 23, 2003, to January 12, 2004, with the amplitude and phase of eight tidal constituents from the Oregon State University tidal prediction software specified at the upper and lower left corners of the ocean boundary, and using the corrections to amplitude and phase for the 1996 historical period. The NOAA predicted tide at Astoria during the same period was subtracted from the simulated time series at Astoria, and the residual was smoothed with a 5-day running average. This provided a small correction (average about 9 cm) to the tidal boundaries to account for unresolved minor tidal harmonics and effects of the geometry of the estuary on the propagation of the tides. The ocean boundary conditions were converted to an hourly time series of elevations, and the smoothed residual was added into those time series, as well as the projected change in mean sea level and the storm surge based on the winter 2007 prototype, to provide the final ocean boundary condition for the future climate simulations.

Adaptive Hydraulics (AdH) Model

Adaptive Hydraulics (AdH) is a multi-physics computer model developed by the USACE, Engineer Research and Development, and Coastal and Hydraulics Laboratory to evaluate hydrodynamics and related transport processes (https://chl.erdc.dren.mil/adh/main/index.html, accessed February 23, 2018). AdH incorporates capabilities for the numerical simulation of saturated and unsaturated groundwater flow, the full Navier-Stokes equation, as well as 2- and 3-dimensional (2- and 3-D) shallow-water equations. The AdH 2D shallow-water equations are based on the vertical integration of the equations of mass and momentum conservation for incompressible flow under the hydrostatic pressure assumption. Reynolds stresses are evaluated using the Boussinesq approach based on the gradient in the currents, fluid density, and kinematic eddy viscosity. The AdH shallow-water equations conserve local and global mass, and balance momentum with pressure across an interface (Berger and Howington, 2002).

The domain is represented by an unstructured triangle mesh where an implicit finite element method (FEM) solves for variables of interest, in this case water depth and velocity. An unstructured mesh allows element size to vary throughout the model domain. The shallow-water equations are discretized using the Petrov-Galerkin FEM approach, with primary variables being represented as linear polynomials across each element (Berger and Stockstill, 1995). Material properties affecting fluid flow due to friction, eddy-viscosity, or other local considerations are assigned for each element based on morphology, vegetation, and if present, relevant physical aspects of structures.

The adaptive feature of AdH consists of its ability to dynamically refine and relax the model mesh and vary temporal resolution such that both model accuracy and model performance are optimized. The ability of AdH to allow the domain to be wet and dry as flow conditions or water depths change is suitable for solving fluid flow problems in shallow marsh environments, beach slopes, flood plains, and other terrain features of interest. For the simulations discussed in this report, the adaptive mesh option was not activated (the AdH mesh remained static through each simulation).

Lower Columbia River Model Development

The AdH model was first developed for the LCR in 2011–12, under a collaborative framework between the USACE-Portland District and the Engineering and Research Development Center-Coastal and Hydraulics Laboratory (Pevey and others, 2012; Savant and McAlpin, 2014) to evaluate the effect of sea-level change on the water-surface profile and sediment transport within the Federal navigation channel, to optimize dredged material management practices within the LCR, and to evaluate hydraulic attributes of several habitat restoration projects.

The LCR AdH model domain extends from Bonneville Dam to 33 km offshore into the Pacific Ocean (fig. 1). The large domain allowed simulation of ocean tide propagation into the Columbia River estuary and LCR, fluvial flow from LCR main stem and tributaries, and tides interacting with riverine flow. The initial model domain had spatial resolution that varied from 10 to 1,000 m, and was represented by approximately 433,300 elements and 226,100 nodes. Nodal point elevations within the AdH model FEM mesh were interpolated from a digital elevation model developed from lidar (Watershed Sciences, 2010) and bathymetric survey data collected by the USACE Portland District. The LCR AdH model uses the 2D shallow water flow module to simulate time-varying depth-averaged currents and time-varying river stage in a horizontally variable framework. The scope for this study focused on evaluating river stage for the Portland-Vancouver area (RM 90–110; fig. 4). Although salinity and related baroclinic (3D) circulation in the Columbia River affects the hydraulics of the lower estuary (RM 0 to 25), salinity effects of the lower estuary have minor effect on river stage in the Portland-Vancouver area, especially during high fluvial discharge periods. For this reason, salinity propagation was not considered relevant for this work, so a 3D analysis to evaluate saline and fresh water mixing was not required. Consequently, model results may be unreliable downstream of RM 25.

Lower Columbia River Model for Climate Change Study

Prior to this study, the LCR AdH model had been used by the USACE for evaluating fluvial flow scenarios equal to or less than the 0.5 AEP. Initial development of the LCR AdH model did not include areas that would be inundated by flows significantly greater than 0.5 AEP. Because the LRC project was focused on evaluating Columbia River flows for future scenarios greater than the current 0.01 AEP in combination with effects of relative SLC, the LCR AdH model was modified and recalibrated for the LRC project. The following model modification tasks were required to improve the AdH model for use on the LRC project:

1. Increase mesh resolution in the lower reaches of inflow tributaries to ensure physically accurate flow conveyance and model stability during extreme high flow conditions.
2. Expand the model mesh coverage to include flood plains that have the potential of being inundated during peak flow conditions evaluated for this project.
3. Expand the mesh coverage to include areas behind levees in order to accurately simulate the effect of interior area storage on the river profile should the levees become overtopped. (The interior areas for several "very high" levees in the Portland metro area, east of PEN 2 along RM 108–120 (fig. 2), were not implemented within the AdH model because it was deemed highly unlikely that these levees would be overtopped in the model simulations. The model accurately defined the crest elevation for these levees (MCDD and SDIC); however, if the simulated river stage exceeded the crest elevation of these levees, the levees would not be overtopped and river stage would continue to increase as if the levee were an infinitely high wall.) Consequently, these levees were not overtopped during model runs for this study. If they had been overtopped, the mesh would have been revised to correctly emulate the levee interior area aspects.
4. Increase mesh resolution to ensure accurate portrayal of levee crest elevation and width.
5. Increase mesh resolution near confluence areas, where multiple channels meet or rejoin, to ensure physically accurate flow conveyance and model stability during extreme high flow conditions. For example, it was essential that Multnomah Channel (fig. 4) be accurately portrayed within the model domain, due to the complex hydraulic connectivity that Multnomah Channel has with the Willamette and Columbia Rivers, and with the flood plain of Sauvie Island during high water conditions.
6. Fully resolve backchannel areas behind diking districts—Smith and Bybee Lakes and the Columbia Slough (fig. 4), for example to ensure physically accurate flow conveyance and model stability during extreme high flow conditions.

After the modifications were imposed on the model, the mesh had increased to 518,000 elements and 268,000 nodes; an increase of 84,700 elements and 41,900 nodes from the inception of the model.

Physical Parameters—Each polygon within the AdH LCR mesh was assigned a material type based on river morphology, such as emergent and upland vegetation, channel thalweg, off-channel flood plain, or pile dike. Hydraulic friction of the terrain was defined in terms of Manning's n values, which were converted to an equivalent bed-roughness height based on water depth and material type. Manning's n varied from a low of 0.015 in the ocean to a high of 0.08 on channel islands (table 5). Turbulent shear stress was defined in term of a constant eddy viscosity, which varied from a low value of 2 in the main channel, to a high of 20 in pile dikes.

Hydraulic Structures—The AdH model included most of the 233 pile dikes in the LCR and numerous levee systems within the model mesh. Rather than emulate each individual piling, the pile dikes were represented within the AdH mesh in terms of average pile density (piles per unit area) applied over the effective area (figs. 12*C* and 12*D*). Pile dikes were expressed as unsubmerged vegetation with a Manning's roughness coefficient of 0.05, pile density equal to 1.5 piles per square meter, and pile diameter of 0.3 m. Pevey and others (2012) documents that this approach successfully emulated pile dikes as compared to expressing each timber element within a pile dike. A disadvantage of emulating pile dikes as unsubmerged vegetation is that top elevation for timber piles is unbounded, regardless of river stage and the pile dike effect may be overestimated for conditions when river stage is significantly higher than the actual pile top elevation; however, this effect is assumed to be small for the LCR due to the high porosity of the simulated pile dikes. The LCR levees also were represented within the AdH mesh with a width of two mesh elements to avoid any numerical "leakage" across unsubmerged levees, and levee height was determined from lidar and construction documentation (table 6).

External Boundary Conditions—The LCR AdH model has two types of hydraulic boundary conditions: (1) a downstream ocean boundary simulated with time-varying water-surface elevation and (2) upstream tributary inflow boundaries for the five main riverine systems simulated with time-varying flow. The farthest downstream ocean boundary of the AdH model is a semi-circular arc extending 33 km offshore from the mouth of the Columbia River. The upstream boundaries of the AdH model are defined by the head of tides for each of the five main riverine systems affecting the model domain.

Time-varying water-surface elevation, based on tides measured by NOAA at the tide gage at Astoria (9439040; RM 17.5), was applied to the ocean boundary of the AdH model at a 1-hour time step for the calibration simulations that used historical data and the climate change scenario evaluations. Because the Astoria tide gage is located 24 km inland and 57 km from the ocean boundary of the model, it was necessary to adjust the measured tide elevations before applying them at the ocean boundary. The tidal adjustment had three parts: vertical shift, amplitude reduction, and time lag. The mean of the measured tidal data at Astoria required a vertical shift of -0.027 m and a scaling factor of 0.95 due to the tidal wave amplification within the estuary. The scaling factor essentially decreases the amplitude of the tidal signal, whereas the vertical shift adjusts the mean of the signal. Due to the distance between the AdH ocean tidal boundary and the Astoria tidal gage, a time lag of 1.1 hours was applied to the Astoria tide data. The resulting simulated water-surface elevation at Astoria closely matched the data reported by NOAA. The tidal adjustment factors were developed as part of the LCR AdH model development (U.S. Army Corps of Engineers, 2016) and followed a similar approach and associated values produced to support the 2014 Columbia River Treaty Study (WEST Consultants, written commun., November 11, 2011).

Boundary conditions for river inflow were applied at each of the five upstream tributary locations using a time-varying flow boundary condition at a 1-day time step. Inflow boundary conditions used USGS data for the Columbia River at Bonneville Dam, Sandy River, Washougal River, Willamette River, Lewis River, and Cowlitz River as described in section, “Hourly Flow Hydrographs at Upstream Boundaries.”

Historical Simulations

The calibration of the LCR hydraulic models focused on adjusting the roughness parameters (table 5) to simulate river stage accurately during high-flow periods in 1996 and 1997. The simulated stage near the mouth of the LCR was compared to NOAA-predicted tidal stage at Astoria, and simulated stage near Portland was compared to measured water-surface elevations in the Columbia River at Vancouver (14144700) and in the Willamette River at Portland (14211720). There were differences in the calibration and validation procedure used for the two models. The Delft3D-FM model was calibrated to Willamette River stage during the winter 1996 flood, whereas the AdH model was calibrated to Columbia River stage during the spring 1997 freshet event in order to bracket the uncertainty in Portland-vicinity flood stage.

The Delft3D-FM model was calibrated to the 1996 flood, with an emphasis on adjusting friction parameters (Chézy coefficients) to accurately simulate the overall flood hydrograph and, in particular, peak stage at the Willamette River stage gage at Portland (14211720). This decision was based on the higher peak stage on the Willamette River at Portland than the stage on the Columbia River at Vancouver, and because this type of flood was exceptional mostly because of the high flows in the Willamette River that coincided with moderately high flows on the Columbia. The Delft3D-FM model was then validated to the 1997 flood, with no change in friction parameters.

In contrast, the AdH model was calibrated to the 1997 flood, with an emphasis on accurately simulating the peak stage on the Columbia River at Vancouver. This decision was made because the Columbia Corridor Levee System is located on the Columbia River and within several miles of Vancouver; therefore, it was more important to match the higher stage at Vancouver on the Columbia River than to match stage at Portland on the Willamette River. Model calibration for the AdH model was achieved by adjusting the hydraulic friction parameters (Manning’s n). Calibration for the AdH model was achieved for the 1997 freshet by increasing the Manning’s-n value for three mesh material types: Material 1 (off-channel area) was increased from 0.025 to 0.0265, Material 3 (river thalweg) was increased from 0.025 to 0.0275, and Material 7 (shore attached riparian/upland) was increased from 0.025 to 0.050. These Manning’s-n adjustments are reasonable because the initial values were based on flows for a 0.5 AEP flood. The higher Manning’s n values used in the current study were necessary because simulated higher flows result in enhanced bedforms and increased riverbed friction (U.S. Army Corps of Engineers, 2014). The AdH model then was validated to the 1996 flood, with no further changes.

Simulations for 1996

This extraordinary high-water event (during January 15–February 28, 1996) was the result of an atmospheric river rain period and the associated rapid increase in temperature, following prolonged snow accumulation at high elevations. The resulting regional (westside of the Cascade Mountains) run-off was characterized by high flow conditions for all LCR tributaries. The flood had an estimated AEP of 0.01 for Willamette River flow and an AEP of 0.05 for the combined flow in the Columbia and Willamette Rivers. Near the mouth of the Columbia River during February 5–10, the combination of a spring phase ocean tide and a coastal storm surge of 0.6 m (2.0 ft) resulted in a sea level at the MCR exceeding 3 m (10 ft) above NAVD 88. Thus, the February 1996 flood affected the LCR water levels from both the ocean and upstream boundaries.

Flow in the Willamette River at Portland (14211720) peaked at 11,800 m^3/s (417,000 ft^3/s) on February 9, 1996, 12–24 hours after the Columbia River peaked at 13,200 m^3/s (466,000 ft^3/s) at Bonneville Dam on February 8, 1996. Considerable effort was expended by the USACE to manage Columbia and Willamette River flood control reservoirs to avert flooding in the Portland-Vancouver metro area. The Willamette River is constrained through urbanized Portland and has a fraction of the hydraulic radius of the Columbia River, and unlike the 1997 freshet in which the Willamette River was essentially a backwater for Columbia River high flow, the Willamette River peak flow during February 1996 was 85-percent of the combined peak flow in the Columbia River downstream of the confluence.

Both models were run for the period between January 15 and February 28, 1996, to capture the hydrograph build-up to the February 8–9 flood and then simulate the slow ramp-down period, and both models captured the trends in Columbia River and Willamette River water-surface elevations at Astoria, Portland, and Vancouver (figs. 13**,** 14**,** and 15). Throughout the 1.5-month simulation, AdH model results tended to be 0.05 to 0.1 m higher than the measurements made at the Columbia River at Vancouver. Delft3D-FM model results over the entire simulation were less biased than AdH model results (-0.022 m [-0.07 ft] as opposed to 0.11 m [0.37 ft], table 7) but the peak stage simulated by the Delft3D-FM model was about 0.3 m (1 ft) lower than measurements, whereas the peak stage simulated by the AdH model was about 0.1 m (0.3 ft) higher (table 8, fig. 15). The comparison between the two models was similar at the Willamette River at Morrison Bridge streamgage—AdH model results were biased high over the entire simulation (0.28 m [0.93 ft]), Delft3D-FM model had a lower bias (0.10 m [0.33 ft]), and the peak stage simulated by the AdH and Delft3D-FM models was 0.39 m (1.29 ft) and 0.11 m (0.37 ft) higher, respectively, compared to the streamgage measurements (table 8). The performance statistics for both models were very good—Nash-Sutcliffe statistics ranged from 0.96 to 0.99 (table 7). Root mean squared error (RMSE) was 0.11 m (0.37 ft) (at Columbia River at Vancouver) and 0.18 m (0.59 ft) (at Willamette River at Morrison Bridge) in Delft3D-FM model simulation results, RMSE was 0.16 m (0.52 ft) (at Columbia River at Vancouver) and 0.32 m (1.06 ft) (at Willamette River at Morrison Bridge) in the AdH model simulation results. Some deviation from measurements at the streamgages is expected and a consequence of simplifying assumptions used in the models. For example, the boundary condition at Bonneville Dam is based on daily-averaged flow and therefore will smooth out some real fluctuations, which could broaden the simulated peak in water-surface elevation downstream. Much of the difference between the model simulation results, however, can be explained by the selections made during the calibration process. The AdH model was calibrated to Columbia River at Vancouver stage during 1997; the Delft3D-FM model was calibrated to Willamette River at Morrison Bridge stage during 1996. It is notable that both models simulated a peak stage during the 1996 flood that was higher at Morrison Bridge than at Vancouver by similar amounts—0.37 m (1.21 ft) in the AdH model, and 0.46 m (1.50 ft) in the Delft model (table 8). The measurements indicated Morrison Bridge peak stage was higher by only 0.059 m. Because both models were calibrated separately but resulted in a similar difference in stage between Portland and Vancouver, the difference is likely due to an incomplete understanding of the hydraulics of the Portland-vicinity system during the 1996 flood or uncertainties in the Willamette River boundary.

The maximum water-surface elevation profiles for the AdH and Delft3D-FM models along the Columbia River were in good agreement from RM 0 to about RM 38 but diverged upstream from there (fig. 16). Upstream of this transition point, the maximum stage simulated by the AdH model was consistently higher than that simulated by the Delft3D-FM model, by an average of 0.45 m (1.48 ft), with the maximum difference of 0.74 m (2.43 ft) occurring about RM 87. The gradient in water-surface elevation in both models also increased upstream of about RM 38. The increase in the gradient of the water-surface profile is consistent with geologic and morphologic confinement of the Columbia River upstream of RM 38, especially under high flow conditions. The AdH maximum water-surface elevation profile was higher than the Delft3D-FM maximum water-surface elevation profile along the entire reach of the Columbia River upstream from RM 38, and the 0.38 m (1.22 ft) difference in maximum water-surface elevation between the two models is evident at RM 105 (Vancouver; fig. 2); however, both models reasonably bound the 1996 high-water marks collected from RM 39 to 114 (table 9; fig. 16).

Several levee systems downstream of the Portland-Vancouver area were overtopped during the 1996 model run in both models. These included Tenasillahe Dike, Lake River Dike, and parts of the Clark County diking district near Ridgefield, Washington. These same levees are thought to have been overtopped during the 1996 flood, based on anecdotal information. The overtopping of these levees and filling of the areas behind them had little or no effect on the water-surface elevation hydrograph at Vancouver because the rate of overtopping was slow and because the storage volume in the flooded interior areas was small compared to the volume of flood water in the LCR.

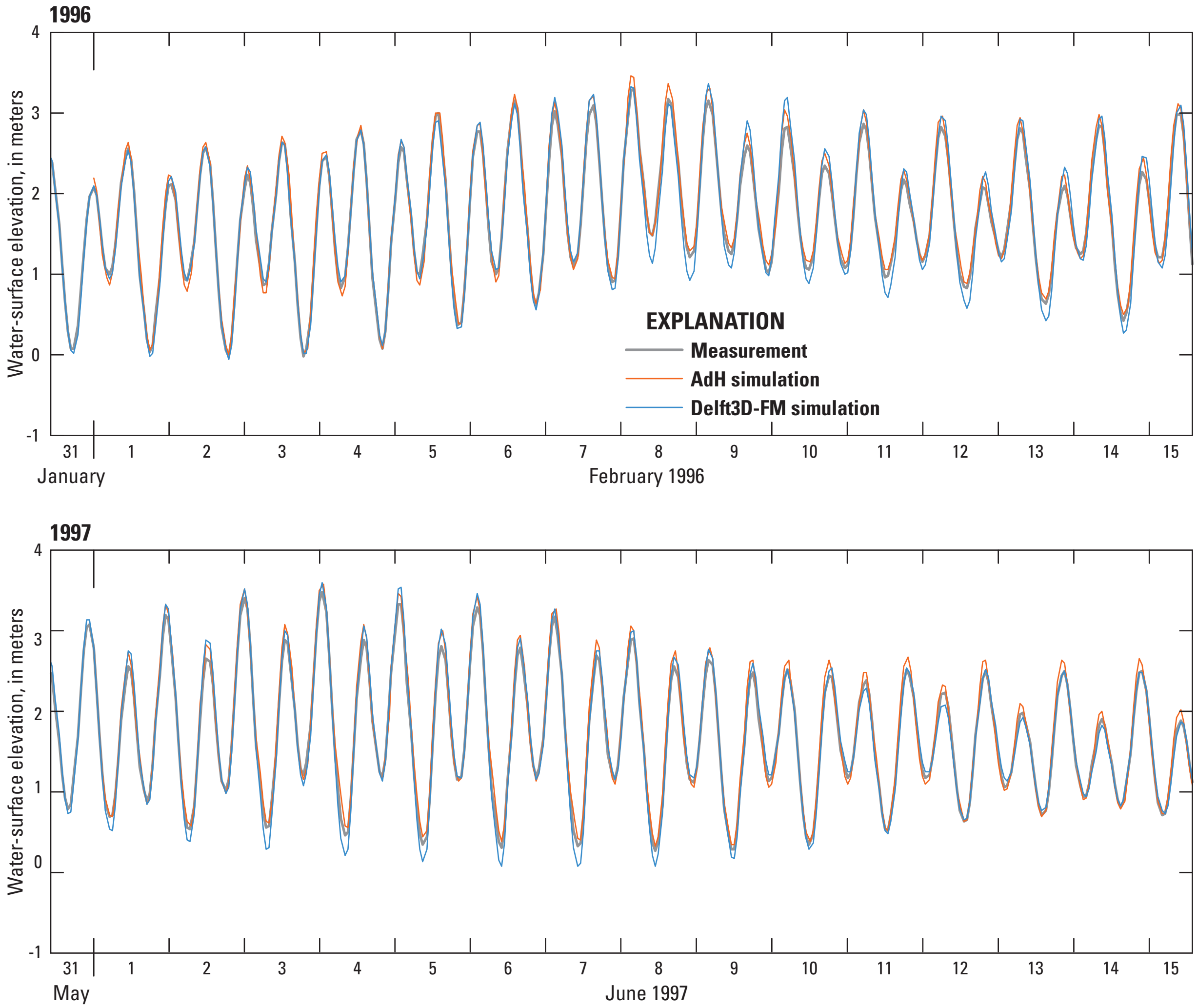

Figure 13. Measured and simulated time series on the Columbia River at Astoria, Oregon, 1996 and 1997.

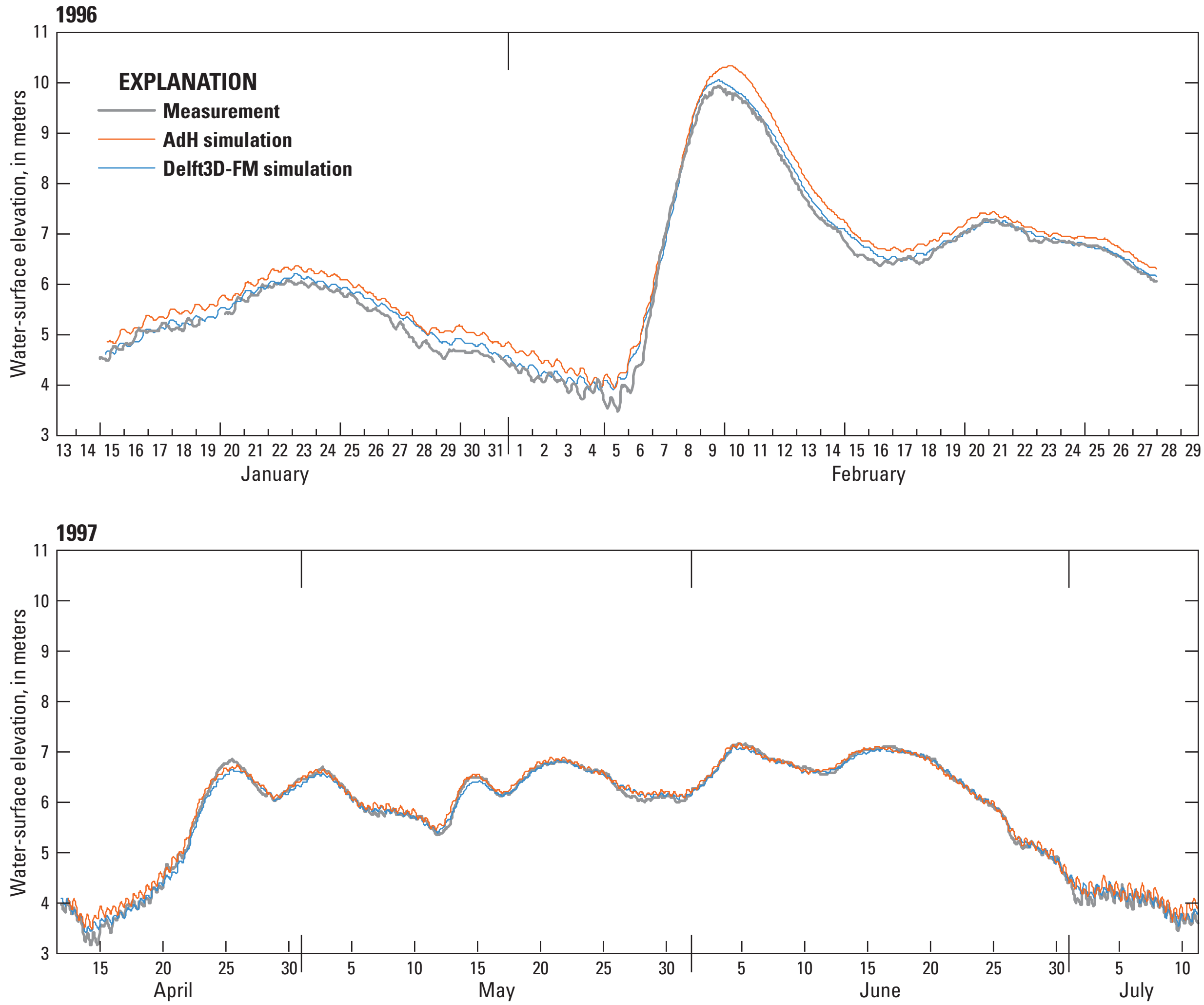

Figure 14. Measured and simulated water-surface elevations at the Willamette River at Morrison Bridge, Oregon, 1996 and 1997.

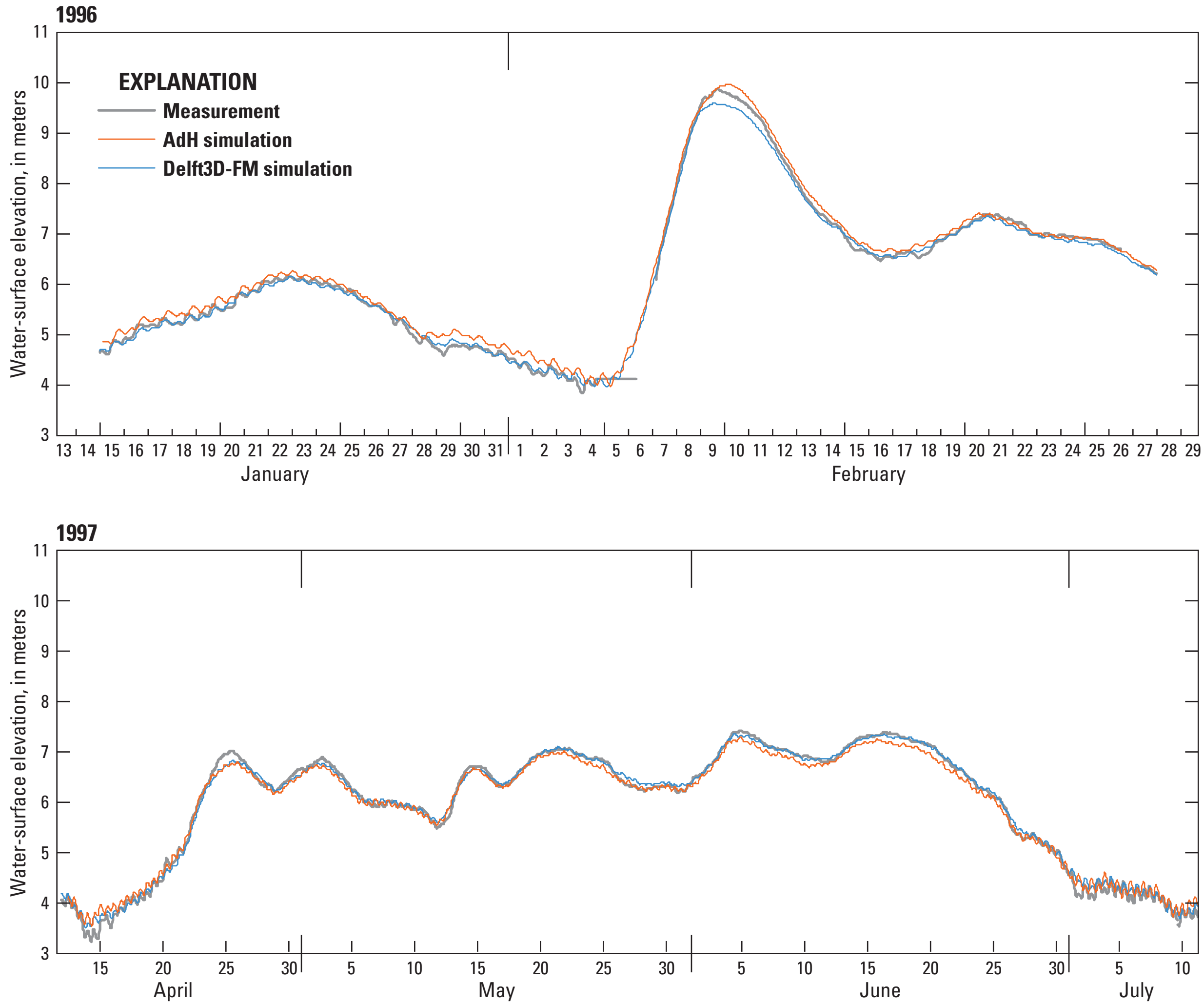

Figure 15. Measured and simulated water-surface elevations at the Columbia River at Vancouver, Washington, 1996 and 1997.

Table 7. Hydraulic model performance statistics, Willamette and Columbia Rivers, Oregon and Washington, 1996 and 1997.

[**Model:** AdH, Adaptive Hydraulics model. Delft3D-FM, Delft3D-Flexible Mesh model. **Abbreviations:** ft, foot; m, meter]

Model	Year	Root mean square error		Nash-Sutcliffe statistic	Bias		Number data points
		(m)	(ft)		(m)	(ft)	
Willamette River at Morrison Bridge, Portland, Oregon (14211720) hourly values							
Delft3D-FM	1996	0.18	0.59	0.99	0.100	0.33	1,057
AdH	1996	0.32	1.06	0.96	0.280	0.93	1,057
Delft3D-FM	1997	0.09	0.28	0.99	0.002	0.01	2,185
AdH	1997	0.13	0.41	0.99	0.065	0.21	2,185
Columbia River at Vancouver, Washington (14144700) hourly values							
Delft3D-FM	1996	0.11	0.37	0.99	-0.022	-0.07	1,057
AdH	1996	0.16	0.52	0.99	0.110	0.37	1,057
Delft3D-FM	1997	0.09	0.29	0.99	0.016	0.05	2,185
AdH	1997	0.13	0.43	0.99	-0.031	-0.10	2,185

Table 8. Comparison of peak stage for historical simulations, Willamette and Columbia Rivers, Oregon and Washington, 1996 and 1997.

[**Model:** AdH, Adaptive Hydraulics model. Delft3D-FM, Delft3D-Flexible Mesh model. **Abbreviations:** ft, foot; m, meter; NAVD, North American Vertical Datum of 1988]

Model	Year	Peak stage above NAVD 88		Deviation of simulated peak stage from measured peak stage	
		(m)	(ft)	(m)	(ft)
Mouth of Columbia River at Tongue Point, Astoria, Oregon (9439040)					
Measured	1996	3.53	11.58	NA	NA
Delft3D-FM	1996	3.76	12.32	0.23	0.74
AdH	1996	3.74	12.26	0.21	0.68
Measured	1997	3.34	10.95	NA	NA
Delft3D-FM	1997	3.60	11.82	0.27	0.87
AdH	1997	3.57	11.70	0.23	0.75
Willamette River at Morrison Bridge, Portland, Oregon (14211720)					
Measured	1996	9.95	32.64	NA	NA
Delft3D-FM	1996	10.06	33.01	0.11	0.37
AdH	1996	10.34	33.94	0.39	1.29
Measured	1997	7.17	23.52	NA	NA
Delft3D-FM	1997	7.11	23.32	-0.062	-0.20
AdH	1997	7.19	23.58	0.016	0.05
Columbia River at Vancouver, Washington (14144700)					
Measured	1996	9.89	32.45	NA	NA
Delft3D-FM	1996	9.60	31.51	-0.29	-0.94
AdH	1996	9.98	32.73	0.085	0.28
Measured	1997	7.43	24.37	NA	NA
Delft3D-FM	1997	7.36	24.14	-0.069	-0.23
AdH	1997	7.30	23.93	-0.13	-0.44
Difference in peak stage between Willamette River at Portland and Columbia River at Vancouver					
Measured	1996	0.059	0.19	NA	NA
Delft3D-FM	1996	0.46	1.50	NA	NA
AdH	1996	0.37	1.21	NA	NA
Measured	1997	-0.26	-0.85	NA	NA
Delft3D-FM	1997	-0.25	-0.82	NA	NA
AdH	1997	-0.11	-0.36	NA	NA

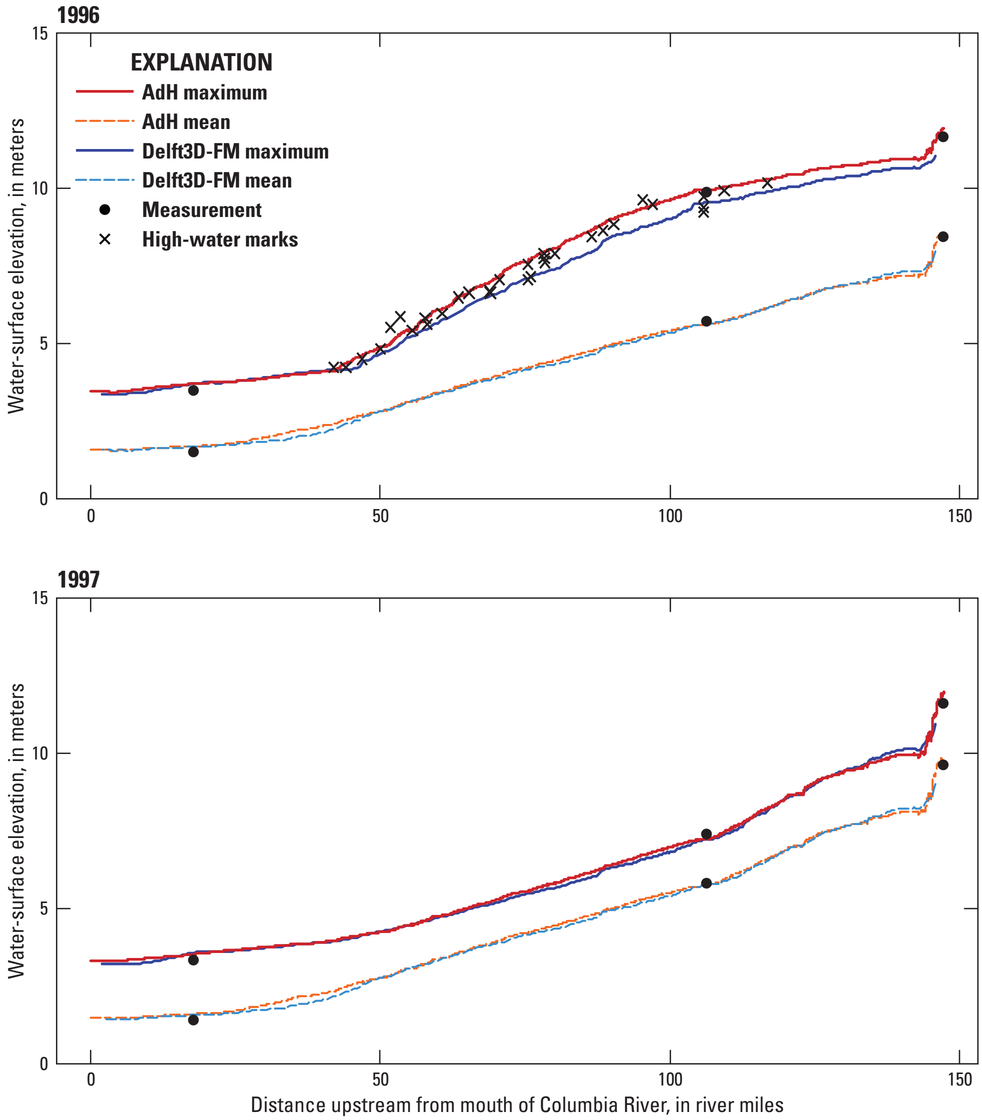

Figure 16. Stream profile showing simulated water-surface elevation, river miles 0–150, Columbia River, Oregon and Washington.

Table 9. High-water marks measured by CH2MHILL for the U.S. Army Corps of Engineers along the Columbia River, Oregon and Washington, February 1996.

[Elevations are in meters above North American Vertical Datum of 1988. Latitude/longitude referenced to North American Datum of 1927. **Abbreviations:** ft, foot; HWM, high-water mark; mi, mile; NA, not applicable; NGVD 29, National Geodetic Vertical Datum of 1929; PGE, Portland General Electric; RM, river mile; USACE, U.S. Army Corps of Engineers; USWB, U.S. Weather Bureau]

River mile	Elevation	Latitude	Longitude	Comment
39.0	4.24	46.190	-123.425	Puget Island; on right bank on northwest side of island, on Ostervold Road, about 1,700 ft from intersection with Crossdike Road and North Welcome Slough Road.
41.1	4.24	46.171	-123.402	Puget Island; on right bank on southwest side of island, at 327 West Sunny Sands Road (near west end of Sunny Sands Road).
43.9	4.52	46.150	-123.365	Puget Island; on right bank at south end of island, off East Sunny Sands Road about 0.8 mi from intersection with Highway 409 (Ferry Road).
47.1	4.82	46.138	-123.296	On left bank on north side of Webb Drainage District Dike Road about 0.85 mi east of Woodson Road.
48.8	5.53	46.135	-123.252	NA
50.5	5.88	46.150	-123.220	NA
52.6	5.43	46.174	-123.190	NA
54.8	5.82	46.172	-123.156	From PGE Beaver Power Plant staff gage, HWM form, and photograph.
55.1	5.62	46.170	-123.149	NA
57.8	5.98	46.168	-123.104	Vicinity of Mayger RM 57.7.
60.5	6.49	46.163	-123.044	Elevation by Cowlitz County Consolidated Diking Improvement District #1.
62.4	6.64	46.141	-123.015	Elevation by Cowlitz County Consolidated Diking Improvement District #1; river staff gage at Reynolds pump station outfall.
66.0	6.69	46.101	-122.965	NA
66.1	6.64	46.108	-122.959	Elevation by Cowlitz County Consolidated Diking Improvement District #1; staff gage on port dock.
67.7	7.05	46.090	-122.933	NA
72.5	7.57	46.040	-122.870	Could be exposed to wave action from Columbia River.
72.6	7.07	46.040	-122.865	Within leveed area north side Kalama River.
73.1	7.18	46.029	-122.887	NA
75.4	7.76	46.007	-122.845	Local ponding east of Interstate 5 in city of Kalama.
75.4	7.90	46.004	-122.847	NA
75.6	7.64	45.996	-122.872	NA
77.2	7.89	45.982	-122.830	NA
83.7	8.46	45.890	-122.806	At Columbia City, Oregon.
85.6	8.64	45.867	-122.799	St. Helens; located north side of St. Helens Marina on side street to right and behind 135 North River Street.
87.4	8.85	45.846	-122.803	HWM established by Boise Cascade Corporation at their St. Helens paper mill plant.
92.4	9.64	45.779	-122.779	Sauvie Island, at north end of Columbia Diking District, HWM on east side of Reeder Road.
94.2	9.50	45.758	-122.771	Sauvie Island, south of Willow Point at Columbia Diking District; HWM on telephone pole on Reeder Road across from Fish and Wildlife grey building.
103.0	9.73	45.646	-122.735	Elevation by Vanalco: staff gage at their dock on Columbia River.
103.0	9.38	45.652	-122.726	Elevation by Vanalco: on south side New River Road; Bonneville Power Administration substation, slough.
103.0	9.25	45.652	-122.725	Elevation by Vanalco: on north side New Lower River Road; that is, Vancouver Lake.
106.5	9.93	45.621	-122.674	At Interstate 5 bridge: USWB and USACE recording gage; stage = 27.15 at 1800, February 9, 1996; datum = 1.82 ft above NGVD 29.
114.0	10.18	45.593	-122.523	HWM (double headed nail on carport/shop wall) set by property owner

Simulations for 1997

During the freshet simulation (April 12–July 12, 1997), the Columbia River main stem was the dominant contributor of flow to the LCR. Streamflow at Bonneville Dam peaked at 16,000 m^3/s (565,000 ft^3/s), which was more than 10 times the peak flow in the Willamette River. Columbia River flow at Bonneville Dam was greater than the 0.3 AEP for 9 continuous weeks and greater than the 0.10 AEP for 6 weeks. For most of the 1997 freshet, the Willamette River at Portland (14211720) was essentially a backwater due to the high flow in the Columbia River. The 1997 freshet tested the AdH and Delft3D-FM models in terms of a long duration and variable high-flow condition with intermittent contributions from LCR tributaries and spring-neap ocean tidal forcing. The maximum water-surface elevation profile along the Columbia River as simulated by both models was in good agreement (fig. 16). The maximum water-surface elevation gradient tended to increase upstream of RM 38 in both models, with an average difference of 0.04 m (0.13 ft) between the two, as the Columbia River estuary narrows and the river becomes fluvially dominated. At the mouth of the Columbia River, the AdH and Delft3D-FM models matched well the measured tidal time series at Astoria (fig. 13). The AdH and Delft3D-FM models also matched the Willamette and Columbia River stage at Portland and Vancouver, respectively, reasonably well through multiple peaks between April and June (figs. 14 and 15). Peak flood stage in both models was lower than measurements at Vancouver by about 0.1 m (0.2 to 0.4 ft), and for the Willamette River at Portland, the AdH model matched the peak flood stage whereas the Delft3D-FM model was lower by about 0.1 m (0.2 ft) (table 8). The performance statistics for both models were very good—Nash-Sutcliffe statistics were consistently 0.99 (table 7). Root mean squared error (RMSE) was 0.09 m (0.3 ft) at Vancouver and Morrison Bridge in Delft model results, RMSE was 0.13 m (0.4 ft) at Vancouver and Morrison Bridge in the AdH model results.

Future Climate Scenarios

Simulations considered three extreme but plausible future boundary conditions which paired scaled-up 1996 inflow hydrographs with an ocean boundary constructed from record high tides, storm surge, and 0-, 0.25-, and 1-m sea-level change (SLC).

The future climate simulations showed similar maximum stage profiles between models along the main channel of the LCR (fig. 17). For all three scenarios, the water-surface elevations in the estuary match well between models and start to diverge upstream. In the 0- and 0.25-m SLC simulations, the divergence between models occurs at around RM 50, similar to the 1996 simulated profile; however, in the 1-meter SLC simulation the divergence occurs at around RM 30. Upstream of RM 50, the AdH simulations were 0.32 to 0.39 m (1.05 to 1.28 ft) higher on average as compared to Delft3D-FM. At the upstream boundary, the difference in maximum stage between the models was consistent across all future simulations, and was consistent with the difference in maximum stage simulated by the two models in 1996 (fig. 16).

The future simulations also were consistent between models at the mouth of the LCR and near Portland. At Astoria, the model simulation results were nearly identical for all future scenarios and simulated peak stages were similar, with the greatest difference between models being 0.07 m (0.23 ft) for the 0-m SLC (fig. 18; table 10). The increase in stage at Astoria from the historical (1996) peak ranged from 1.13 to 2.11 m (3.71 to 6.93 ft) (table 10), reflecting the cumulative effects of higher SLC at the ocean boundary. In both the Willamette and Columbia Rivers, the future simulations had good agreement between the AdH and Delft3D-FM models with respect to the timing and magnitude of floods (figs. 19 and 20). In the Willamette River, the difference in peak stage between the two models ranged from 0.06 to 0.07 m (0.17 to 0.24 ft) for the three future climate simulations, and increases from the historical (1996) peak ranged from 1.69 m (5.56 ft) seen in the 0-m SLC scenario to 1.90 m (6.24 ft) in the 1-m SLC scenario (table 10). Therefore, the increase in stage simulated for future climate scenarios compared to the measured 1996 peak stage is significantly larger than the differences between the two models. The difference in peak stage between the two models was greater in the Columbia River at Vancouver, ranging from 0.24 to 0.29 m (0.80 to 0.93 ft) across the three future climate simulations, which was similar in magnitude to the difference between peak stage simulated at Vancouver by the two models in the 1996 simulations. The increase in stage from the historical peak in the Columbia River ranged from 1.26 m (4.13 ft) in the 0-m SLC scenario to 1.65 m (5.40 ft) in the 1-m SLC scenario; again, larger than the difference between the two models (fig. 20; table 10).

The peak stage information was compared to known levee elevations to determine if overtopping occurred in any of the future scenario simulations. The PEN 1 levee along the Columbia River was designed to a top elevation of 11.80 m (38.71 ft) upstream and 11.73 m (38.48 ft) downstream; however, USACE lidar data indicated that the low point actually is 11.07 m (36.32 ft) above NAVD 88. Therefore, the levee is overtopped by at least 0.08 m (0.26 ft) for the 0-m SLC scenario (Delft3D-FM model simulation results) and by as much as 0.47 m (1.54 ft) for the 1-m SLC scenario (AdH model simulation results; fig. 20). The PEN 2 levee along the Columbia River was designed to a top elevation of 11.86 m (38.91 ft) upstream and 11.73 m (38.49 ft) downstream, above NAVD 88; however, USACE lidar data indicated the low point actually is 11.48 m (37.67 ft) above NAVD 88. Therefore, the levee is at incipient overtopping (table 10; fig. 20). Neither the MCDD nor SDIC levee systems overtopped during the future climate simulations.

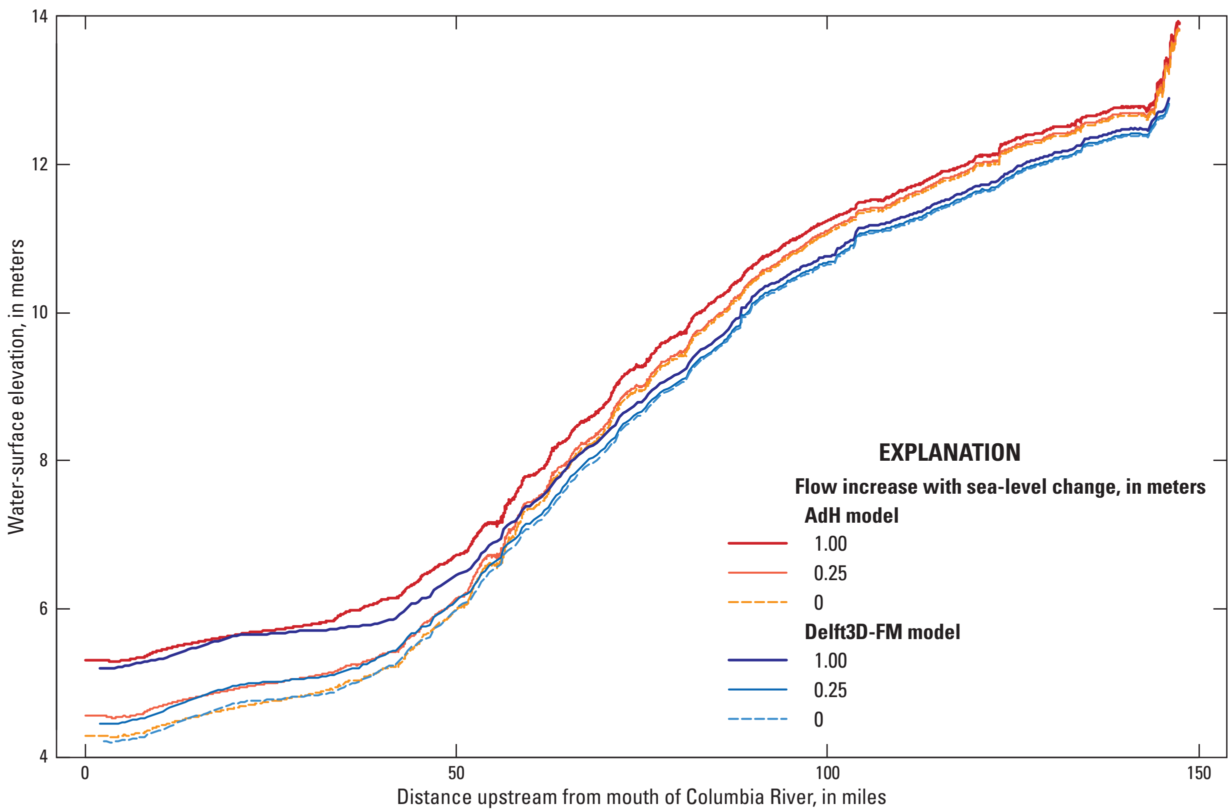

Figure 17. Stream profile showing future simulated maximum river stage from AdH and Delft3D-FM models along the Columbia River, Oregon and Washington.

Additionally, the duration of high water levels on levees is expected to increase. In the 1-m SLC scenario, the AdH-modeled river stage exceeding 11.5 m (37.7 ft) at the location of MCDD levees is estimated to have a duration of 6–9 hours, whereas water levels exceeding 11 m (36 ft) may be sustained for 2 days through the course of the rise and fall of water levels. The 1996 measured peak stage was 9.89 m (32.45 ft) at the Columbia River at Vancouver (14144700; table 10) with stage exceeding 8 m (26 ft) for 5 days, and the high sustained stage after the 1996 peak was a little less than 8 m (26 ft) for 11 days. In the future climate scenarios, river stage is expected to be greater than 8 m (26 ft) for 21 days (fig. 20). This type of flood will test the Columbia Corridor Levee System both in terms of the capacity of levees to prevent overtopping and their ability to resist failure due to seepage.

To create the future boundary conditions hydrographs on which these simulations are based, historical 1996 flows were scaled up by a factor of 1.4 at Bonneville Dam, and by a factor of 1.2 on the Willamette River and all other tributaries. Even though the prototype flow selected was a historical rain-on-snow event in which the Willamette River flows had a lower AEP than the Columbia River, it was not a certainty that, when the boundary conditions were scaled in this way, the water-surface elevation gradient would be downward between Portland and Vancouver. Based on our simulations, the resulting water-surface elevation was higher in the Willamette River at Portland by 0.3 m (1 ft) (AdH model simulation results) to 0.5 m (1.6 ft) (Delft model simulation results), than on the Columbia River at Vancouver. Therefore, in terms of the boundary conditions and hydraulics near the confluence, the future extreme flood simulated bears more resemblance to the atmospheric river rain-on-snow period in 1996, than to the spring freshet of 1997 in which the Willamette River was essentially a backwater to the Columbia River. This contributes to significant hydraulic complexity around the North Portland Peninsula between the Columbia and Willamette Rivers, and the Multnomah Channel. Simulations indicated that the Multnomah Channel conveyed much flow and contributed to significant flooding at Sauvie Island.

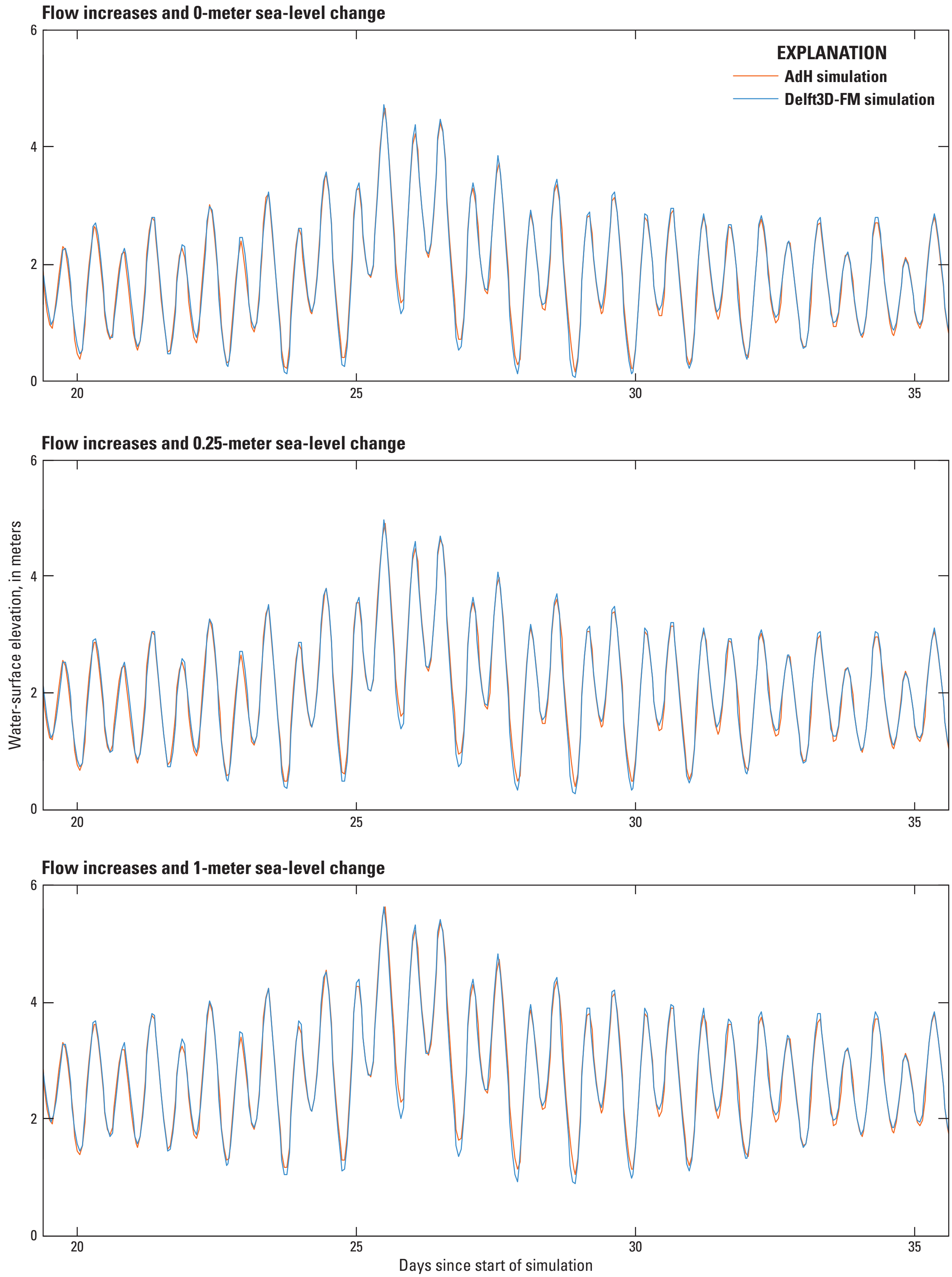

Figure 18. Simulated future water-surface elevations from AdH and Delft3D-FM models, Columbia River at Astoria, Oregon.

Table 10. Measured historical and simulated future peak stage and projected sea-level change for selected areas in the Willamette and Columbia Rivers, Oregon and Washington.

[**Model:** AdH, Adaptive Hydraulics model. Delft3D-FM, Delft3D-Flexible Mesh model. **Abbreviations:** ft, foot; m, meter; NA, not applicable; NAVD 88, North American Vertical Datum of 1988]

Model	Sea-level change (m)	Peak stage in NAVD 88		Increase in peak stage from historical measurement	
		(m)	(ft)	(m)	(ft)
Columbia River at Astoria, Oregon (9439040)					
Measured in 1996	NA	3.53	11.58	NA	NA
Delft3D-FM	0.00	4.73	15.52	1.20	3.94
AdH	0.00	4.66	15.29	1.13	3.71
Delft3D-FM	0.25	4.97	16.30	1.44	4.72
AdH	0.25	4.92	16.13	1.39	4.55
Delft3D-FM	1.00	5.64	18.51	2.11	6.93
AdH	1.00	5.64	18.51	2.11	6.93
Willamette River at Morrison Bridge, Portland, Oregon (14211720)					
Measured in 1996	NA	9.95	32.64	NA	NA
Delft3D-FM	0.00	11.64	38.20	1.69	5.56
AdH	0.00	11.70	38.37	1.75	5.73
Delft3D-FM	0.25	11.68	38.32	1.73	5.68
AdH	0.25	11.74	38.50	1.79	5.86
Delft3D-FM	1.00	11.78	38.65	1.83	6.00
AdH	1.00	11.85	38.89	1.90	6.24
Columbia River at Vancouver, Washington (14144700)					
Measured in 1996	NA	9.89	32.45	NA	NA
Delft3D-FM	0.00	11.15	36.58	1.26	4.13
AdH	0.00	11.39	37.38	1.50	4.93
Delft3D-FM	0.25	11.18	36.67	1.29	4.22
AdH	0.25	11.43	37.50	1.54	5.05
Delft3D-FM	1.00	11.25	36.92	1.36	4.47
AdH	1.00	11.54	37.85	1.65	5.40

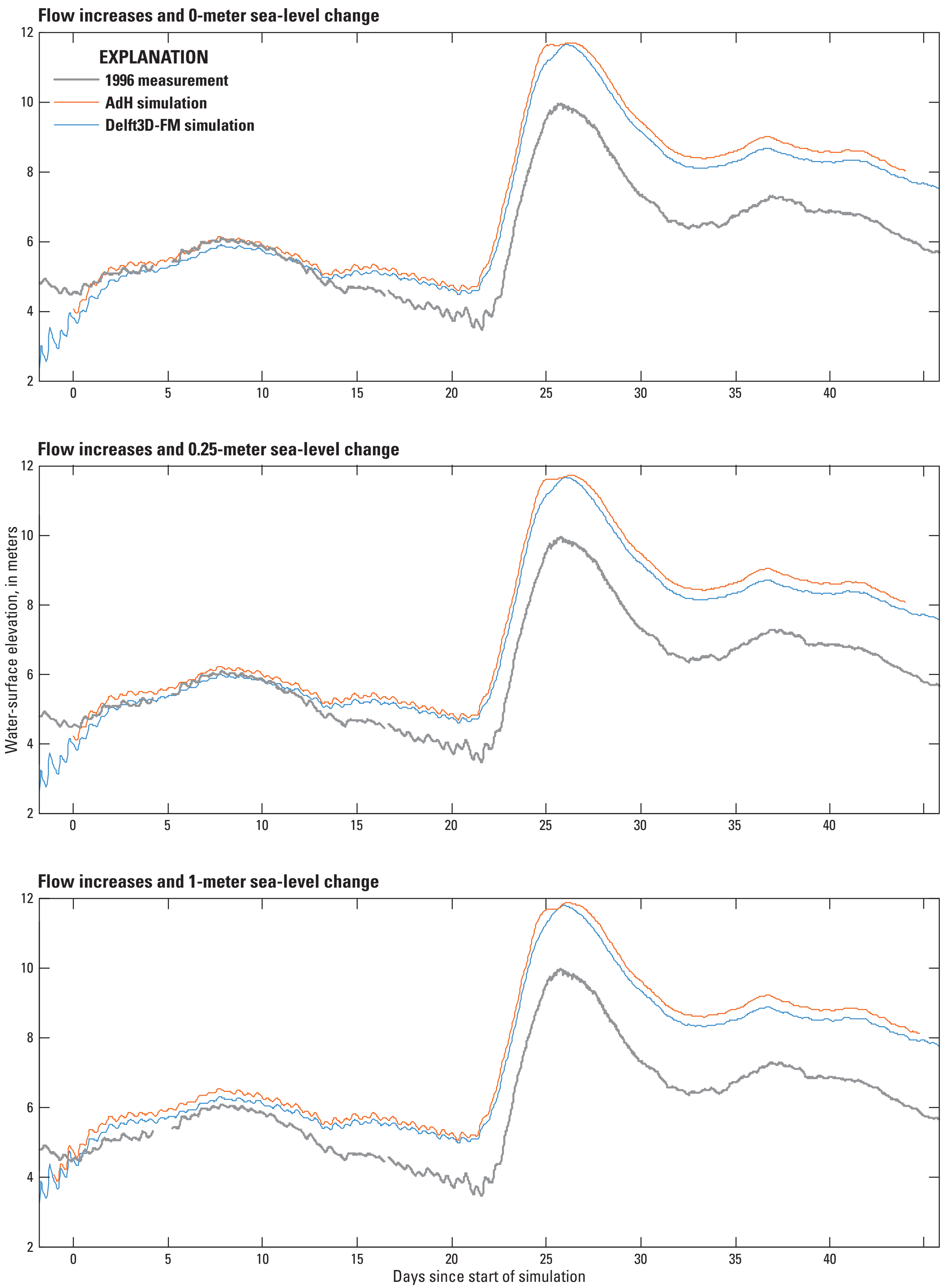

Figure 19. Measured historical and simulated future water-surface elevations from AdH and Delft3D-FM models, Willamette River at Morrison Bridge, Oregon.

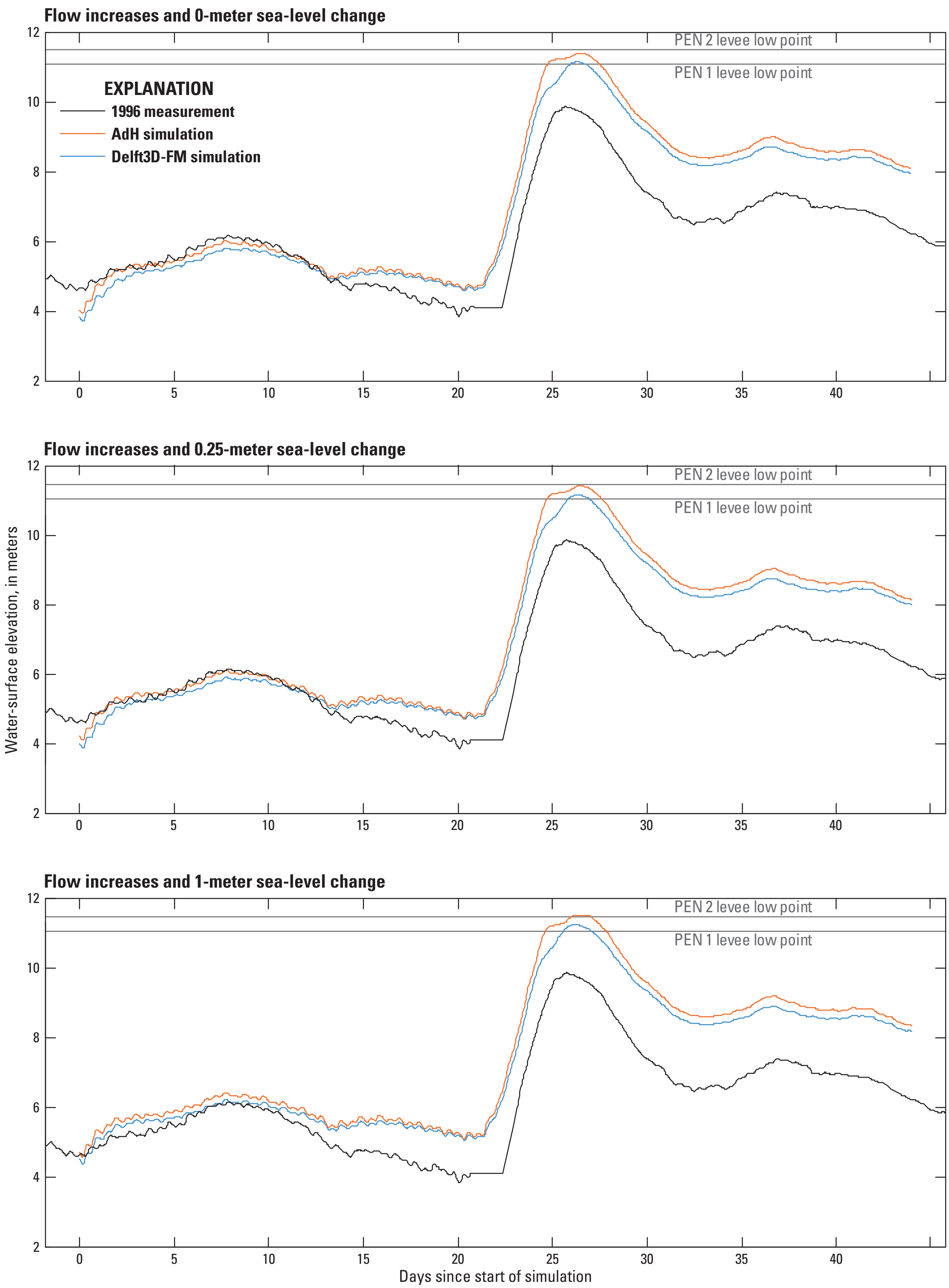

Figure 20. Measured historical and simulated future water-surface elevations from AdH and Delft3D-FM models, Columbia River at Vancouver, Washington.

Summary and Conclusions

This study provided important information for the Levee Ready Columbia project and the Columbia Corridor Levee System in the Portland, Oregon, area regarding the potential effect of a future climate on extreme but plausible floods. The lower estuary of the Columbia downstream of river mile 40 is the most affected by ocean conditions, including a change in mean sea level. Under even some relatively extreme assumptions, the change in mean sea level will not have a large effect on the flood stage in Portland; an increase of 0.25 meters in mean sea level changed the simulated peak stage at Portland by only 3–4 centimeters (1–2 inches). A large storm surge, however, can have a larger effect on the flood stage at Portland because the storm surge can add up to 1.4 meters (4.6 feet) of water-surface elevation at the ocean boundary. A large storm surge in combination with high flows associated with a winter storm is not a remote possibility as the atmospheric rivers that cause rain-on-snow winter floods in the Willamette River Basin often are associated with storm surges at the coastline. If circumstances are particularly adverse, high storm surge can be associated with a high spring tide, which can add another few meters to ocean water-surface elevation. Therefore, when considering an extreme but plausible high flow in Portland, it is prudent to consider a storm surge and high tide at the ocean occurring in concert.

Nonetheless, the reach of the Columbia River along Peninsula Drainage District No. 1 and No. 2 in Portland is fluvially dominated. Under the assumptions made in this study about future Columbia Basin hydrology, based on the best available scientific data and professional judgment, extreme high-flow boundary conditions were imposed in the models. The selected critical events were a winter streamflow in the Columbia River that was modeled as 40-percent greater than current conditions and an extreme winter streamflow in the Willamette River resulting from a rain-on-snow type of flow could be about 20-percent greater than current conditions. Under the selected future climate scenarios, most levees in the LCR will be subject to prolonged exposure from water levels that exceed the authorized levee height making the Columbia Corridor Levee System vulnerable to such high flood stage from increased flows on the Columbia and Willamette Rivers.

There is significant hydraulic complexity in the area near the confluence of the Columbia and the Willamette Rivers, and where the Multnomah Channel leaves the Willamette River. The Multnomah Channel conveys much flow from the Willamette River under the assumed future climate scenarios. This complexity warrants additional study in order to understand the effects of flooding, particularly on Sauvie Island. The conveyance of the Multnomah Channel also affects the water-surface profile in the main channel of the Columbia River between Portland and St. Helens, Oregon.

It is important, to correctly account for flood plain storage, that levees be overtopped in the simulations in a realistic manner. This requires that levee-crest elevations be defined as accurately as possible, not just in the Portland area, but in the entire lower Columbia River. There may still be unresolved uncertainty in some levee heights along this reach.

There is a benefit to using different models developed by independent teams to investigate such a complex simulated flood stage on the Columbia from Bonneville Dam to the Pacific Ocean. This approach provides independent verification of results and provides clarity about whether the results are robust enough to be well outside any differences that can be ascribed to the particular model selected. The range in results also provides an estimate of uncertainty.

Two state-of-the-art hydraulic models—Adaptive Hydraulics (AdH) and Delft3D-Flexible Mesh (Delft3D-FM)—were used to simulate the same extreme but plausible peak flood in the future, to assess the sensitivity of the results and conclusions. The models differed in how physical structures such as levees and pile dikes were embedded into the numerical mesh, in the mesh resolution, in how friction was parameterized, and the measurements given the most weight in the calibration phase. Great care was taken, however, to assure that bed elevation in the two model meshes was based on the same terrain model, that levee heights and access to interior storage were the same, and that the models were run with the same boundary conditions. The domain of both models included the Columbia River between Bonneville Dam and the Pacific Ocean, and the Willamette River between Willamette Falls and the confluence with the Columbia River, as well as the lowest reaches of three small tributaries. Although the domain included the ocean boundary and estuary, the models were run in two dimensions and did not consider salinity and three-dimensional circulation in the estuary because the effects on stage at the Columbia Corridor Levee System were negligible during high flows in the fluvially dominated study reach.

Both models simulated the 1996 winter rain-on-snow storm, and the 1997 spring freshet, and accurately matched the timing of floods in the fluvially dominated reach of the rivers and the tidal effects on the water-surface elevation in the estuary, during both historical periods. The AdH model was calibrated with an emphasis on simulating the water-surface elevation of the Columbia River at Vancouver (14144700; RM 105) during the 1997 spring freshet. The Delft3D-FM model was calibrated with an emphasis on simulating the water-surface elevation of the Willamette River at Portland (14211720) during the 1996 winter flood. Based on comparison to water-surface elevations at Columbia and Willamette River streamgages at Vancouver and Portland, the models had comparable and good performance statistics over the two historical periods. For the AdH model, the Nash-Sutcliffe statistic ranged from 0.96 to 0.99, the RMSE from 0.13 to 0.32 m (0.41 to 1.06 ft), and the bias from -0.03 to 0.28 m (-0.10 to 0.93 ft). For the Delft3D-FM model, the Nash-Sutcliffe statistic was 0.99, the RMSE ranged from 0.09 to 0.18 m (0.28 to 0.59 ft), and the bias from -0.02 to 0.10 m (-0.07 to 0.33 ft). Considering only the highest peak-flood stage simulated in 1996, the AdH model simulated

9.98 m (32.73 ft), the Delft3D-FM model simulated 9.60 m (31.51 ft), and the measured peak stage was 9.89 m (32.45 ft) at the Columbia River at Vancouver (U.S. Geological Survey streamgage 14144700). At the Willamette River at Portland (14211720), the AdH model simulated a peak stage of 10.34 m (33.94 ft), the Delft3D-FM model simulated 10.06 m (33.01 ft), and the measured peak stage was 9.95 m.

In the 1996 simulations, the peak stage simulated by the AdH model was higher than that simulated by the Delft3D-FM model throughout the main channel upstream of the estuary. At about RM 38 an inflection point indicated a transition in the Columbia River from being tidally dominated to being fluvially dominated. Upstream of this transition point, the maximum stage simulated by the AdH model was consistently higher than that simulated by the Delft3D-FM model, by an average of 0.45 meters, with the maximum difference of 0.74 meters occurring about RM 87. In the 1997 simulations, the average difference in maximum stage between the two models along the reach upstream of RM 38 was only 0.04 meters. This difference in simulated peak stage along the channel is likely explained by a combination of factors including the effect of differences in meshes in how off-channel storage is simulated, differences in friction properties resulting from how friction is parameterized in the two models, differences in sites used in model calibration, and differences in how the two models simulate pile dikes. The Delft3D-FM model simulates pile dikes as impermeable weirs with a fixed height that can be overtopped, whereas the AdH model simulates pile dikes within the mesh cells as porous regions with higher roughness that cannot be overtopped.

The calibrated models were used to simulate extreme but plausible high water in the near future—2030 to 2059—which is identified as the 2040s. Both models were applied using a scenario-based approach, consistent with U.S. Army Corps of Engineers and U.S. Geological Survey practice for evaluating future conditions affected by climate change. The analyses are based on the best available scientific data and professional judgment, but there is inherent uncertainty in hydrologic and coastal conditions when simulating future water-surface profiles in the Columbia River.

The future scenarios represent simulated large-scale climate trends which are extreme but plausible at the regional scale, assumptions about what type of event will be most important in the future, and appropriate coincident tidal and storm surge conditions. The use of scenarios informs adaptive management by placing management actions in a context of future uncertainty and by bounding the envelope of potential climate effects.

This study used projected future climate results, and uncertainties documented in reports on future climate published in 2010 through present by regional agencies. These studies focused on the 2040s timeframe and developed streamflow datasets in collaboration with University of Washington Climate Impacts Group. The forecasted climate change datasets were used to develop boundary conditions for three future scenarios incorporating increases in river flow and relative sea-level rise.

The literature also points to changing Columbia River basin hydrology on time scales relevant to infrastructure planning. Projected future trends indicate an earlier peak in the spring freshet is likely on the main stem, shifted on average by about 1 month, from a May to June peak in current conditions to a late April to early May peak in the 2040s. Concurrently, increases in winter (November–March) runoff volume in the Willamette Valley are plausible as well. Although the future spring Columbia River peak stage would not coincide with the stage of Willamette River winter flows, the rise on the Columbia River would begin earlier, effectively increasing 2040s winter discharges in the Columbia River at the time of the peak flow on the Willamette River. This pointed to a February 1996 type winter rain-on-snow event as being more likely to cause plausible extreme future floods than the spring freshet.

The 2040s relative change in sea level at Astoria, Oregon, was estimated to vary between -0.015 to 0.25 meter above North American Vertical Datum of 1988 (NAVD 88) based on U.S. Army Corps of Engineers guidance. Storm surge and high-tide conditions based on regional observations were aligned so that the timing of sea-level peaks were appropriately shifted from the timing of water-level peaks near Portland, and added to future sea level. Storm surge and tidal conditions were determined to have a more significant effect on the coastal boundaries than projected sea-level change.

The future 2040 condition hydraulic model inflows were amplified compared to the baseline measured historical flows. For modeling purposes, it was estimated that a winter peak on the Columbia River could be as much as 40-percent higher and on the Willamette River could be as much as 20-percent higher than the February 1996 historical winter flood that was used as a prototype.

Forcing the hydraulic models with plausible extreme future inflows at the upstream boundaries and a combination of 0.25 meter of sea-level change, extreme storm surge and high tides at the ocean boundary resulted in a 2040s stage of 11.4 meters (37.5 feet) and 11.2 meters (36.7 feet) on the Columbia River at Vancouver (14144700) for the AdH and Delft3D-FM models, respectively. The two models generally agreed well, and both showed peak stages more than 1 meter higher than the peak stage measured in 1996. Under the selected future climate scenarios, it was also evident that levees generally will be subject to more prolonged exposure to high water levels.

The hydraulic analyses revealed that the lower Columbia River estuary, from the mouth to approximately river mile 38, was the reach most affected by the tidal and storm surge conditions and change in mean sea level. From Columbia River mile 38 and upstream, fluvial discharges, as expected, had a dominant influence on the water-surface elevations adjacent to the Columbia Corridor Levee System between river miles 105 and 145.

Results from this study indicate that a 1996-type flood, perturbed by the selected future climate-change scenario, can subject Multnomah County Drainage District (MCDD) levees to a peak water level exceeding 11 meters (36 feet) above NAVD 88 and a long-duration river level of 8 meters (26 feet) above NAVD 88. The AdH- and Delft3D-FM-modeled 2040s peak stage, with flow increases and a sea-level change of 1.00 meter, is 11.5 and 11.25 meters (37.9 and 36.9 feet) on the Columbia River at Vancouver (14144700), respectively. In this scenario, the peak AdH-modeled river stage exceeding 11.5 meters (37.9 feet) at the location of MCDD levees is estimated to have a duration of 6–9 hours, whereas river levels exceeding 11 meters above NAVD 88 may be sustained for 2 days through the course of the rising and falling water levels. The 1996 measured peak stage was 9.9 meters (32.5 feet) above NAVD 88 at the Columbia River at Vancouver (14144700), and the high sustained stage after the 1996 peak was just under 8 meters (26 feet). In the future climate scenarios, river stage is expected to be more than 8 meters (26 feet) above NAVD 88 for 21 days. This type of flow will test the Columbia Corridor Levee System both in terms of the capacity of levees to prevent overtopping and their ability to resist failure due to seepage.

Acknowledgments

This study supported efforts by Levee Ready Columbia and was funded by the following partners: Peninsula Drainage District No. 1, Peninsula Drainage District No. 2, Multnomah County Drainage District No. 1, Sandy Drainage Improvement Company, Cities of Portland, Gresham, Fairview, and Troutdale, Multnomah County, Metro, and the Port of Portland. This project was funded in part with a financial award from the Special Public Works Fund and Regional Solutions, funded by the Oregon State Lottery and administered by the Oregon Infrastructure Finance Authority.

References Cited

Berger, R.C., and Howington, S.E., 2002, Discrete fluxes and mass balance in finite elements: Journal of Hydraulic Engineering, v. 128, no. 1, p. 87–92, https://doi.org/10.1061/(ASCE)0733-9429(2002)128:1(87).

Berger, R.C., and Stockstill, R.L., 1995, Finite-element model for high-velocity channels: Journal of Hydraulic Engineering, v. 121, no. 10, p. 710–716, https://doi.org/10.1061/(ASCE)0733-9429(1995)121:10(710).

Bonneville Power Administration, 2004, 2000 Level Modified Streamflow 1928–1999—Diversion and Return Flow Patterns, Summation of Depletion Adjustments, Evaporation Adjustments, 2000 Level Modified Streamflow—Columbia and Coastal Basins: Portland, Oregon, Bonneville Power Administration report.

Brekke, L., Keupper, B., and Vaddey, S., 2010, Climate and Hydrology Datasets for use in the RMJOC agencies' longer-term planning studies—Part I, Future climate and hydrology datasets, Bureau of Reclamation report, accessed September 28, 2018, https://www.usbr.gov/pn/climate/planning/reports/index.html.

Cayan, D.R., 1996, Interannual climate variability and snowpack in the western United States: Journal Climate, v. 9, p. 928–948.

Climate Impacts Group, 2009, The Washington Climate Change Impacts Assessment, *in* McGuire Elsner, M., Littell, J., and Whitely Binder, L., eds., Center for Science in the Earth System, Joint Institute for the Study of the Atmosphere and Oceans: Seattle, Washington, University of Washington, http://www.cses.washington.edu/db/pdf/wacciareport681.pdf.

Climate Impacts Group, 2018, Resources—Climate Impacts Group datasets: University of Washington database, accessed March 9, 2018, at https://cig.uw.edu/resources/data/cig-datasets/.

Deltares, 2015, D-Flow Flexible Mesh—D-Flow FM in Delta Shell user manual (ver. 1.1.148, rev. 43108): The Netherlands, Deltares, 402 p.

Egbert, G.D., and Erofeeva, S.Y., 2002, Efficient inverse modeling of barotropic ocean tides: Journal of Atmospheric and Oceanic Technology, v. 19, no. 2, p. 183–204, https://doi.org/10.1175/1520-0426(2002)019<0183:EIMOBO>2.0.CO;2.

Elias, E.P.L., Gelfenbaum, G., and Van der Westhuysen, A.J., 2012, Validation of a coupled wave-flow model in a high-energy setting—The mouth of the Columbia River: Journal of Geophysical Research—Oceans, v. 117, C09011, 21 p., doi:10.1029/2012JC008105.

Fox, D.S., Bell, S., Nehlsen, W., and Damron, J., 1984, The Columbia River Estuary atlas of physical and biological characteristics: Astoria, Oregon, Columbia River Estuary Data Development Program, 87 p.

General Bathymetric Chart of the Oceans, 2018, Gridded bathymetry data: International Hydrographic Organization (IHO) and the Intergovernmental Oceanographic Commission database, accessed March 13, 2018, at https://www.gebco.net/data_and_products/gridded_bathymetry_data/.

Granato, G.E., 2009, Computer programs for obtaining and analyzing daily mean streamflow data from the U.S. Geological Survey National Water Information System website: U.S. Geological Survey Open-File Report 2008–1362, 123 p. on CD-ROM, 5 appendixes.

Groisman, P.Y., and Easterling, D.R., 1994, Variability and trends of total precipitation and snowfall over the United States and Canada: Journal of Climate, v. 7, no. 1, p. 184–205, https://doi.org/10.1175/1520-0442(1994)007<0184:VATOTP>2.0.CO;2.

Hamlet, A.F., Elsner, M.M., Mauger, G.S., Lee, S.Y., Tohver, I., and Norheim, R.A., 2013, An overview of the Columbia Basin Climate Change Scenarios Project—Approach, methods, and summary of key results: Atmosphere-ocean, v. 51, no. 4, p. 392–415, https://doi.org/10.1080/07055900.2013.819555.

Hamlet, A.F., and Lettenmaier, D.P., 1999, Effects of climate change on hydrology and water resources in the Columbia River Basin: Journal of the American Water Resources Association, v. 35, no. 6, p. 1597–1623, https://doi.org/10.1111/j.1752-1688.1999.tb04240.x.

Helaire, L.T., 2016, Modeling of historic Columbia River flood impacts based on Delft 3D simulations: Portland State University, Master of Science thesis, 165 p., accessed January 2018 at https://pdxscholar.library.pdx.edu/open_access_etds/3206/, doi:10.15760/etd.3197.

Hinkel, J., Jaeger, C., Nicholls, R.J., Lowe, J., Renn, O., and Peijun, S., 2015, Sea-level rise scenarios and coastal risk management: Nature Climate Change, v. 5, no. 3, p. 188–190, https://doi.org/10.1038/nclimate2505.

Interagency Advisory Committee on Water Data, 1981, Guidelines for determining flood flow frequency: U.S. Geological Survey Bulletin 17B of the Hydrology Subcommittee, 28 p. plus 14 apps.

Intergovernmental Panel on Climate Change, 2000, Emissions scenarios—A special report of working group III of the Intergovernmental Panel on Climate Change: New York, Cambridge University Press, 608 p.

Intergovernmental Panel on Climate Change, 2007: Climate change 2007—Synthesis report—Contribution of working groups I, II and III to the Fourth Assessment Report of the Intergovernmental Panel on Climate Change: Geneva, Switzerland, Intergovernmental Panel on Climate Change, 104 p.

Intergovernmental Panel on Climate Change, 2014, Climate change 2014—Synthesis report—Contribution of working groups I, II and III to the Fifth Assessment Report of the Intergovernmental Panel on Climate Change: Geneva, Switzerland, Intergovernmental Panel on Climate Change, 151 p.

Jarrett, J.T., 1976, Tidal Prism-Inlet relationships, general investigation of tidal inlets—Report 3: Vicksburg, Mississippi, U.S. Army Engineer Research Center and U.S. Army Engineer Waterways Experiment Station, 55 p.

Liang, X., 1994, A two-layer variable infiltration capacity land surface representation for general circulation models: Seattle, University of Washington, Water Resources Series, TR140, 208 p.

Mote, P.W., and Salathé, E.P., Jr., 2010, Future climate in the Pacific Northwest: Climatic Change, v. 102, no. 1–2, p. 29–50, https://doi.org/10.1007/s10584-010-9848-z.

Mote, P.W., Snover, A.K., Capalbo, S.M., Eigenbrode, S., Glick, P., Littell, J.S., Raymondi, R., and Reeder, S., 2014, Northwest, Chap. 21 *in* Melillo, J., Terese, Richmond, T.C., and Yohe, G.W., eds., Climate change impacts in the United States, The Third U.S. National Climate Assessment: U.S. Global Change Research Program, 16-1-nn.

Orem, H.M., 1968, Discharge in the Lower Columbia River basin, 1928–65: Geological Survey Circular 550, 24 p.

Pevey, K., Savant, G., Moritz, H., and Childs, E., 2012, Lower Columbia River Adaptive Hydraulics (AdH) model—Development, water surfaces elevation validation and sea level rise analysis: Portland, Oregon, U.S. Army Corps of Engineers, Northwest Division, 81 p.

R Core Team, 2016, R—A language and environment for statistical computing: Vienna, Austria, R Foundation for Statistical Computing, https://www.R-project.org/.

Rupp, D.E., Abatzoglou, J.T., Hegewisch, K.C., and Mote, P.W., 2013, Evaluation of CMIP5 20th century climate simulations for the Pacific Northwest USA: Journal of Geophysical Research, D, Atmospheres, v. 118, no. 19, p. 10884–10906, https://doi.org/10.1002/jgrd.50843.

Savant, G., and McAlpin, T.O., 2014, Tidal hydrodynamics in the lower Columbia River estuary through depth averaged adaptive hydraulics modeling: Journal of Engineering, v. 2014, Hindawi Publishing Corporation, article ID 416914, 12 p., http://dx.doi.org/10.1155/2014/416914.

Simenstad, C.A., Burke, J.L., O'Connor, J.E., Cannon, C., Heatwole, D.W., Ramirez, M.F., Waite, I.R., Counihan, T.D., and Jones, K.L., 2011, Columbia River Estuary Ecosystem Classification—Concept and application: U.S. Geological Survey Open-File Report 2011-1228, 54 p., https://doi.org/10.3133/ofr20111228.

Stephenson, A.G., 2016, Harmonic analysis of tides using tide harmonics: The R Foundation, https://CRAN.R-project.org/package=TideHarmonics.

Stewart, I.T., Cayan, D.R., and Dettinger, M.D., 2005, Changes toward earlier streamflow timing across Western North America: Journal of Climate, v. 18, no. 8, p. 1136–1155, https://doi.org/10.1175/JCLI3321.1.

Talley, L.D., Pickard, G.L., Emery, W.J., and Swift, J.H., 2011, Gravity waves, tides, and coastal oceanography, chap. S8 *of* Descriptive physical oceanography—An introduction 6th ed.: Boston, Academic Press, p. 223–244.

Taylor, K.E., Stouffer, R.J., and Meehl, G.A., 2012, An overview of CMIP5 and the experiment design: Bulletin of the American Meteorological Society, v. 93, no. 4, p. 485–498, https://doi.org/10.1175/BAMS-D-11-00094.1.

Tohver, I., Hamlet, A.F., and Lee, S.-Y., 2014, Impacts of 21st century climate change on hydrologic extremes in the Pacific Northwest region of North America: Journal of American Water Resources Association, v. 50, no. 6, p. 1461–1476, doi:10.1111/jawr.12199.

U.S. Army Corps of Engineers, 1948, Review report on Columbia River and tributaries, appendix L—Columbia River below Yakima River: U.S. Army Corps of Engineers, Portland District, 340 p., https://www.streamnetlibrary.org/?page_id=895.

U.S. Army Corps of Engineers, 1991, Review of flood control Columbia River Basin—Columbia River and Tributaries Study, CRT-63, Final Report: U.S. Army Corps of Engineers, North Pacific Division.

U.S. Army Corps of Engineers, 1997, February 1996 post flood report—Hydrometeorlogical evaluation: U.S. Army Corps of Engineers, Portland District, Hydrologic, Coastal, and River Engineering Section.

U.S. Army Corps of Engineers, 2010, Lower Columbia River digital terrain model: Prepared by David Smith and Associates, Inc., David Evans and Associates, Inc., and CC Patterson and Associates for U.S. Army Corps of Engineers, Portland District, Contract No W9127N-09-D-009, Task Order No. 0005, available at http://www.estuarypartnership.org/lower-columbia-digital-terrain-model.

U.S. Army Corps of Engineers, 2014, Columbia River Treaty 2014/2024 review program: U.S. Army Corps of Engineers, Northwestern Division.

U.S. Army Corps of Engineers, 2016, Investigation of impacts associated with modifying east Sand Island to prevent nesting of double-crested cormorants: Vicksburg, Mississippi, U.S. Army Engineer Research and Development Center-Coastal and Hydraulics Laboratory, Technical Report ERDC/CHL TR-15-16.

U.S. Army Corps of Engineers, 2018, Climate preparedness and resilience: U.S. Army Corps of Engineers website, accessed February 27, 2018, at https://www.usace.army.mil/corpsclimate/.

Van der Steeg, S., 2016, Investigations of tidal hydrodynamics in the lower Columbia River and estuary: The Netherlands, Delft University of Technology, Master's thesis, 130 p.

Warner, M.D., Mass, C.F., and Salathé, E.P., Jr., 2015, Changes in winter atmospheric rivers along the North American west coast in CMIP5 climate models: Journal of Hydrometeorology, v. 16, no. 1, p. 118–128, https://doi.org/10.1175/JHM-D-14-0080.1.

Watershed Sciences, 2010, Lidar remote sensing data collection—Columbia River Survey—Final delivery, September 22, 2010: Submitted to Jacob Macdonald, U.S. Army Corps of Engineers, Portland District, by Watershed Sciences, 70 p.

Publishing support provided by the U.S. Geological Survey
Science Publishing Network, Tacoma Publishing Service Center

For more information concerning the research in this report, contact the
Director, Oregon Water Science Center
U.S. Geological Survey
2130 SW 5th Avenue
Portland, Oregon 97201
https://www.usgs.gov/centers/or-water

Wherry and others—**Columbia and Willamette River Flood Stage, Columbia Corridor Levee System at Portland, Oregon, in a Future Climate**—Scientific Investigations Report 2018–5161

ISSN 2328-0328 (online)
https://doi.org/10.3133/sir20185161